

# 國立交通大學

物理研究所

碩士論文

淺穿地球之 tau 微中子模擬研究

A monte-carlo study on earth-skimming tau  
neutrinos

研究生：容震軒

指導教授：林貴林 教授

中華民國 93 年 7 月

# A monte-carlo study on earth-skimming tau neutrinos

研 究 生：容震軒

Student : Chan-Hin Iong

指導教授：林貴林

Advisor : Guey-Lin Lin

國立交通大學

物理研究所

碩 士 論 文



Submitted to Institute of Physics  
College of Science

National Chiao Tung University

in partial Fulfillment of the Requirements

For the Degree of

Master

in

Institute of Physics

June 2004

Hsinchu, Taiwan, Republic of China

# 致謝

謹以此碩士論文獻給於 1995 年病逝的母親，因為她是最會因為我的努力而高興的人。在我小時候母親就常常展現出堅強不屈的個性，她的處事態度總是積極而抱持希望的。甚至在生命的最後關頭，仍能忍耐病痛堅持工作。她使我明白到，就算是面對再大的痛苦，也要堅強地完成該做的事。在她的教育下，養成了我能吃苦及樂於面對挑戰的個性，也影響我對待人生的態度，所以母親是對我很重要決定影響最為關鍵的人。

在求學過程中，我一直認為除了學術成就外，高尚的品格也是成為高等知識份子的必要條件。而學習科學理論可以使頭腦得以訓練，具有好的思考能力後，才能把各種道理想通，這是我求學的主要動機。對我而言，指導教授林貴林老師是良好的榜樣，林老師能彈性接受別人的看法，但對肯定的原則問題卻十分堅持，這都是了解道理的表現。在做研究的過程中，林老師提供很多寶貴的意見，也給我很大的思考自由，而不是要求我服從他的指令，林老師使工作變得十分有趣。

而四年前當我還在中研院工作時，黃明輝老師是最早帶我做物理研究的，每次討論都讓我學到處理數據的技巧，在他用心的指導下，使我在進入研究所前就掌握了很多數值模擬的知識，所以我才能輕鬆地面對現在的研究工作。感謝林老師和黃老師的幫助，使本論文能順利完成。

除了研究所期間的老師外，還要感謝幾位大學時候的老師，因為他們對我當時的學習十分重要。成大機械系林大惠教授讓我在大學二年級時參與實驗工作，使我體會到經過理想化的理論與實驗的差別，也讓我明白到讀書跟做研究的差別，對我日後的學習方法有很大的影響。數值方法是做研究的有力工具，在成大機械系何清政教授的數值分析課程中，擁有豐富數值分析經驗的何老師常強調各種數值方法的特點及使用時可能面對的問題，讓我在初學時就建立了正確觀念。在大學四年級時，何老師帶我做了一年的數值熱流論文，在何老師嚴謹的研究態度下，讓我對研究過程有初步了解。在修科學思維方法時認識了成大數學系陳珍漢教授，之後還學習了陳老師的張量分析及柘樸學。陳老師很強調學習數學的樂趣和對美感的欣賞力。其實念了大學三年的我已累積了一些學習上的價值觀問題，一直難以求證。但陳老師在課堂上往往能說出我的心底話，在我心裡存在很久的問題幾乎一一找到了答案。陳老師讓我明白到不只要學表面的知識，還要找出隱藏在字裡行間的道理，這樣才能把知識轉化到不同專業的應用上，這啟發我日後把不同領域的學問都視為相通的概念。

對我這個年輕探索者而言，毫無疑問以上的老師們對我影響深遠，在此我要再一次感謝他們。

# Contents

<b>1</b>	<b>Introduction</b>	<b>2</b>
<b>2</b>	<b>Monte-carlo method</b>	<b>2</b>
2.1	Random variable . . . . .	3
2.2	Cross section and probability . . . . .	3
2.3	Mapping from the random number . . . . .	4
2.4	Expectation value . . . . .	5
2.5	Fraction of energy loss $y$ . . . . .	6
2.6	Poisson (decay) process . . . . .	6
2.7	General decay process . . . . .	8
2.8	Total energy loss . . . . .	9
2.9	Tau-lepton Range . . . . .	11
<b>3</b>	<b>Process for <math>\nu_\tau</math> and <math>\tau</math></b>	<b>12</b>
3.1	Process for $\nu_\tau$ . . . . .	12
3.2	Process for $\tau$ . . . . .	13
<b>4</b>	<b>Tau-lepton energy loss</b>	<b>15</b>
4.1	Deterministic approach . . . . .	15
4.2	Stochastic approach . . . . .	16
4.2.1	Hard-term energy loss . . . . .	17
4.2.2	Soft-term energy loss . . . . .	18
<b>5</b>	<b>Simulation results</b>	<b>18</b>
<b>6</b>	<b>Discussion</b>	<b>32</b>
<b>7</b>	<b>Conclusion</b>	<b>47</b>



# 1 Introduction

Tau neutrinos can be detected when they skim the Earth and produce tau-leptons. One can identify the  $\nu_\tau$  source by measuring the  $\tau$  energy. For the single energy  $\nu_\tau$  source, the produced tau-lepton energy is predicted to be unique when we apply the deterministic method. In reality, it should be an energy spectrum. We present our Monte-carlo simulation results on tau-lepton energy spectrum induced by the Earth-skimming tau neutrinos, taking into account the inelasticity of neutrino-nucleon scatterings and the tau-lepton energy loss in detail. We argue that the tau-lepton flux resulting from neutrino-nucleon scatterings inside the earth is controlled by the tau-lepton range, rather than the distance of tau-leptons/neutrinos traverse inside the Earth. We also comment on the energy-resolution of tau neutrinos in the earth-skimming detection strategy.

In Sec. 2, we discuss the basic concepts of Monte-carlo method, and the strategy for calculating the energy loss and decay processes. In Sec. 3, we introduce the processes relevant to the propagations of  $\nu_\tau$  and  $\tau$  inside the Earth. In Sec. 4, we compare the difference between deterministic method and the Monte-carlo method for the description of energy loss. In Sec. 5, we summarize our simulation results, including the tau-lepton energy spectra arising from incident  $\nu_\tau$  with different energies. In Sec. 6, we analyze the simulation results, and establish the relationship between the  $\nu_\tau \rightarrow \tau$  conversion rate and the medium thickness. Sec. 7 is the conclusion.

## 2 Monte-carlo method

Usually, an analytic solution of a problem is deterministic. It provides an exact solution for a set of given initial or boundary conditions. Furthermore, some numerical algorithms are developed from this deterministic skill. Therefore, we can obtain a unique solution by this type of numerical method.

On the contrary, Monte-carlo method treats a physical problem as a stochastic process. It involves some random variables to construct the stochastic world. Why do we choose this strategy? It is because some processes are better described in this way. In

section 4.2, we consider the tau-lepton energy loss in a medium as a stochastic process. In this situation, energy loss is a function of random numbers. Hence energy loss is a random variable as well. Consequently, we expect to obtain different energy loss for the same initial tau-lepton energy. Although some variables are created by random numbers, it is important to note that they must satisfy a distribution function, to be described in Sec 2.3.

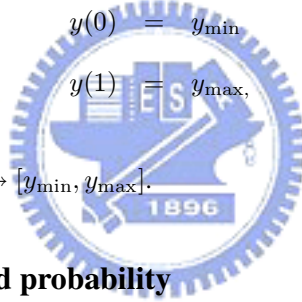
## 2.1 Random variable

The characteristics of Monte-carlo method is the random number. Some variables in Monte-carlo method are no longer deterministic. Let us generate a random number  $r \in [0, 1]$  and an arbitrary variable  $y(r)$  depending on it,

$$y(0) = y_{\min} \quad (1)$$

$$y(1) = y_{\max}, \quad (2)$$

it is a mapping :  $[0, 1] \rightarrow [y_{\min}, y_{\max}]$ .



## 2.2 Cross section and probability

We describe the interaction probability in the medium by the differential cross section  $\frac{d\sigma}{dy}$  with  $y$  the inelasticity of the collision and the total cross section,

$$\sigma = \int_{y_{\min}}^{y_{\max}} \frac{d\sigma}{dy} dy. \quad (3)$$

Note that the total cross section  $\sigma$  may not be 1. In order to normalize it, one can divide  $\sigma$  by itself,

$$1 = \frac{\sigma}{\sigma} = \int \frac{d\sigma}{\sigma dy} dy = \int \frac{dP}{dy} dy = \int dP, \quad (4)$$

where  $dP = \frac{d\sigma}{\sigma}$  is normalized and  $\frac{dP}{dy}|_{y=y_0}$  is the probability for an event with  $y \in [y_0, y_0 + dy]$ .

### 2.3 Mapping from the random number

Let  $r \in [0, 1]$  is a generated random number, we need to design a mapping from the random number  $r$  to the variable  $y$ . An event occurs more easily if it occupies a larger random number range  $dr$ . Although we have not defined the concept of probability, let us consider a mapping given as follows :

$$dr = k \frac{d\sigma}{dy} dy, \quad (5)$$

where  $k$  is a unknown constant. Integrating this relation gives

$$r = \int_0^r dr' = k \int_{y_{\min}}^y \frac{d\sigma}{dy'} dy'. \quad (6)$$

Let us require the following:

$$\text{for } y = y_{\min}, \quad r = k \int_{y_{\min}}^{y_{\min}} \frac{d\sigma}{dy'} dy' = 0, \quad (7)$$

$$\text{for } y = y_{\max}, \quad r = k \int_{y_{\min}}^{y_{\max}} \frac{d\sigma}{dy'} dy' = k \cdot \sigma = 1. \quad (8)$$

The 2nd equation holds if  $k = 1/\sigma$ . Therefore,

$$r = \frac{1}{\sigma} \int_{y_{\min}}^y \frac{d\sigma}{dy'} dy'. \quad (9)$$

This relation means that we can obtain the random number  $r$  corresponding to a given  $y$ , by integrating the differential cross section  $\frac{d\sigma}{dy}$ . It is easy to construct a table for  $r$  in numbers of  $y$ . From this table, one obtains a  $y$  from an arbitrary random number  $r$ . We have said that

$$\frac{dP}{dy} \equiv \frac{1}{\sigma} \frac{d\sigma}{dy} \quad (10)$$

is the differential probability. From Eqs. (5) and (9),

$$dr = \frac{dP}{dy} dy \quad (11)$$

and

$$r = \int_{y_{\min}}^y \frac{dP}{dy'} dy'. \quad (12)$$

The condition  $r = 1$  for  $y = y_{\max}$  implies

$$\int_{y_{\min}}^{y_{\max}} \frac{dP}{dy'} dy' = \frac{1}{\sigma} \int_{y_{\min}}^{y_{\max}} \frac{d\sigma}{dy'} dy' = 1. \quad (13)$$

We have shown that the total probability for the range  $[y_{\min}, y_{\max}]$  is 1. Hence

$$P \equiv \int_{y_1}^{y_2} \frac{dP}{dy'} dy' \quad (14)$$

is the probability for the events with  $y \in [y_1, y_2]$ .

We still need to confirm that  $dr$  is proportional to the area of integral under  $\frac{dP}{dy}$ . From Eq. (11), an infinitesimal area of square  $dr$  is the product of  $\frac{dP}{dy}$  and  $dy$ . Because the area of square is in proportion to its width and height,

$$dr \propto dy, \quad (15)$$

$$dr \propto \frac{dP}{dy}, \quad (16)$$

thus, the range of random number is proportional to the differential probability  $\frac{dP}{dy}$ . We remark that  $\frac{dP}{dy}$  is a function of  $y$ . As we generate a random number  $r$  between 0 and 1, it is apparent that we are more likely to obtain a  $y$  whose  $\frac{dP}{dy}$  is larger.

## 2.4 Expectation value

The expectation value of  $y$  is defined as follows:

$$\langle y \rangle = \int_{y_{\min}}^{y_{\max}} y \frac{dP}{dy} dy. \quad (17)$$

In general, we obtain the expectation value by integrating  $y \frac{dP}{dy}$  directly. On the other hand, Monte-carlo method provides another way to do that.

In order to apply the Monte-carlo method, one must generate sufficient events. The events number needed depends on the type of system. The more events we have, the



more accuracy we achieve. For an individual event, we create a random number  $r_i$ . In section 2.3, we have introduced the method for finding the  $(r_i, y_i)$  table from  $\frac{dP}{dy}$ . For a given random number  $r_i$ , there is a correspondence  $y_i$ . Assuming that we generate  $N$  events, the expectation value  $\langle y \rangle$  is just the average of  $y_i$ ,

$$\langle y \rangle = \sum_{i=1}^N \frac{y_i}{N}. \quad (18)$$

We have transformed the problem from the integral of  $y \frac{dP}{dy}$  to the sum of  $y_i/N$ .

## 2.5 Fraction of energy loss $y$

Let us define the physical meaning of  $y$ . For a particle with an initial energy  $E$ , its energy is changed to  $E'$  after one step of interaction. The fraction of difference between  $E$  and  $E'$  is

$$y = \frac{E - E'}{E}, \quad (19)$$

i.e.,  $y$  is the fraction of particle energy loss. The expectation value  $\langle y \rangle$  can be estimated by Eq. (17) in a deterministic process. Although different values for  $y$  are possible, we only obtain its expectation value. After several steps of interaction, the total energy loss is also a definite value.

Strictly speaking,  $y$  should be considered as a random variable in the Monte-carlo method. Each time we create a random number  $r$ , the random variable  $y$  is obtained by Eq. (9), or by the  $(r_i, y_i)$  table from Sec. 2.3. Consequently, the total energy loss resulting from several steps of interaction is no longer a definite value.

## 2.6 Poisson (decay) process

Let us assume that a process  $N = \{N_i\}$  denotes the numbers of interaction in  $i$  steps. It is called a Poisson process when it holds the following properties.

1.  $N_i$  is an positive integer.
2. For integers  $i, s > 0$ ,  $N_{i+s} - N_i$  is independent of  $\{N_u; u \leq i\}$ .

3. For integers  $i, s > 0$ ,  $N_{i+s} - N_i$  is independent of  $i$ .

Therefore, the interaction of Poisson process is independent of the past history, and also the survival probability. For a particle runs in a distance  $x$ , its survival probability  $P_d^c$  can be written as the form

$$P_d^c = e^{-\frac{x}{L}}, \quad (20)$$

where  $L$  is the interaction thickness. The interaction (decay) probability is

$$P_d = 1 - P_d^c = 1 - e^{-\frac{x}{L}}. \quad (21)$$

The differential decay probability is

$$\frac{dP_d}{dx} = \frac{1}{L} e^{-\frac{x}{L}}. \quad (22)$$

It is normalized already because

$$\begin{aligned} \int_0^\infty \frac{dP_d}{dx} dx &= \frac{1}{L} \int_0^\infty e^{-\frac{x}{L}} dx \\ &= -\left( \lim_{x \rightarrow \infty} e^{-\frac{x}{L}} - e^{-\frac{0}{L}} \right) \\ &= 1. \end{aligned} \quad (23)$$

As we show in Sec. 2.3, the mapping from random number  $r$  to  $x$  is

$$\begin{aligned} r &= \int_0^x \frac{dP_d}{dx'} dx' \\ &= \frac{1}{L} \int_0^x e^{-\frac{x'}{L}} dx' \\ &= 1 - e^{-\frac{x}{L}}, \end{aligned} \quad (24)$$

for  $r \in [0, 1]$  and  $x \in [0, \infty)$ . It is the same to write as

$$r = e^{-\frac{x}{L}}, \quad (25)$$

or

$$x = -L \cdot \log r, \quad (26)$$

since only the relation between  $dr$  and  $dx$  is crucial. If we always obtain a random number in the higher probability region of  $x$ , this mapping should be satisfied that  $\Delta r$  is a monotonous decreasing function on  $x$ ,

$$\Delta r = r(x + \varepsilon) - r(x) = e^{-\frac{x+\varepsilon}{L}} - e^{-\frac{x}{L}}. \quad (27)$$

By comparing  $\Delta r$  of the difference regions of  $x$ , that is  $x' = x + \alpha$ , where  $\alpha > 0$ .

$$\begin{aligned} \Delta r' &= e^{-\frac{x+\alpha+\varepsilon}{L}} - e^{-\frac{x+\alpha}{L}} \\ &= e^{-\frac{\alpha}{L}} (e^{-\frac{x+\varepsilon}{L}} - e^{-\frac{x}{L}}) \\ &= e^{-\frac{\alpha}{L}} \Delta r \end{aligned} \quad (28)$$

Since  $\alpha > 0$ ,  $e^{-\frac{\alpha}{L}} < 1$ , then  $\Delta r' < \Delta r$ . This shows that  $\Delta r$  is a monotonous decreasing function on  $x$ . From now on, we can generate a random number  $r$ , and obtain the position of interaction with Eq. (26). This is applicable to neutrino-nucleon interactions. In the situation of Poisson process, this method reduces the computing time because we do not need to use the step by step method shown in Sec. 2.7. We can obtain the decay position  $x$  straightforwardly by substituting a random number  $r$  to Eq. (26).

## 2.7 General decay process

In general, the tau-lepton decay is not a Poisson process since the tau-lepton energy changes rapidly as it interacts in the medium. The tau-lepton survival probability is no longer given by Eq. (20). We should choose a step by step method rather than solving Eq. (26). When the step size  $\Delta x$  is small enough comparing with the decay length  $D$ , we can make the following approximation by the Taylor series,

$$P_d = 1 - P_d^c = 1 - e^{-\frac{\Delta x}{D}} \approx 1 - (1 - \frac{\Delta x}{D}) = \frac{\Delta x}{D}.$$

The differential decay probability is

$$dP_d = \frac{dx}{D}, \quad (29)$$

where  $D$  is the decay length given by

$$D = C_d \cdot \frac{E}{10^6 \text{ GeV}}, \quad (30)$$

$C_d = 48.9$  m and  $E$  is the energy of the tau-lepton. The tau-lepton decay length is 48.9 m when its energy is  $10^6$  GeV.

## 2.8 Total energy loss

Here we give the definition of a stochastic energy loss process  $E = \{E_n; n \in \mathbb{N}\}$  for  $n$  steps. We assume that the probability is independent of the past history,

$$P\{E_{n+1} = j | E_0, \dots, E_n\} = P\{E_{n+1} = j | E_n\}. \quad (31)$$

The probability of getting  $E_{n+1} = j$  depends on  $E_n$  only. We can rewrite the probability in a simple form,

$$P\{E_{n+1} = j | E_n = i\} \equiv P(i, j), \quad (32)$$

a transition matrix for the  $n$ -th step to  $(n + 1)$ -th step. The energy relation of the  $n \rightarrow n + 1$  step is

$$E_{n+1} = (1 - y)E_n,$$

where  $y$  is the random number, depending on the type of the energy loss. Consider there are only two steps,

$$E = \{E_0, E_1, E_2\},$$

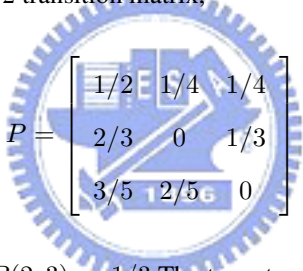
the energy after the first and second step should be

$$\begin{aligned} E_1 &= (1 - y_1)E_0 \\ E_2 &= (1 - y_2)E_1 = (1 - y_2)(1 - y_1)E_0. \end{aligned}$$

Let us consider a particle which has initial energy  $E_0 = a_0$  and goes through a stochastic process. After two steps of energy loss, its energy is reduced to  $E_2$ . For a stochastic system, the probability that we obtain  $E_2 = a_2$  is

$$\begin{aligned} P\{E_2 = a_2 | E_0 = a_0\} &= \sum_{a_1 \in E} P(a_0, a_1)P(a_1, a_2) \\ &\equiv P^2(a_0, a_2). \end{aligned} \quad (33)$$

For example, we have a  $2 \times 2$  transition matrix,



$$P = \begin{bmatrix} 1/2 & 1/4 & 1/4 \\ 2/3 & 0 & 1/3 \\ 3/5 & 2/5 & 0 \end{bmatrix},$$

where  $P(1, 1) = 1/2$  and  $P(2, 3) = 1/3$ . The two steps transition matrix  $P^2$  can be obtained from  $P$ ,

$$P^2 = \begin{bmatrix} 17/30 & 9/40 & 5/24 \\ 8/15 & 3/10 & 1/6 \\ 17/30 & 3/20 & 17/60 \end{bmatrix}.$$

In a general  $n$ -step case, the probability for  $E = a_n$  after the particle going through  $n$ -step of energy loss is

$$\begin{aligned} P\{E_n = a_n | E_0 = a_0\} &= \sum_{a_1, a_2, \dots, a_n} P(a_0, a_1)P(a_1, a_2) \cdots P(a_{n-2}, a_{n-1})P(a_{n-1}, a_n) \\ &\equiv P^n(a_0, a_n). \end{aligned} \quad (34)$$

The quantity  $P^n(a_0, a_n)$  is the probability for a particle to decrease its energy from  $a_0$  to  $a_n$ . In the same way, we have  $P^n(a_0, a'_n), P^n(a_0, a''_n) \cdots$ . This means that we

have a range for  $E_n$  from a single initial energy  $E_0$ . In other words, by Monte-carlo method, we shall obtain a distribution rather than a single value for the final-state energy.

## 2.9 Tau-lepton Range

In general, we define the  $\tau$  range as

$$\langle X \rangle = \sum_{x'} x' P\{X = x'\}, \quad (35)$$

where  $P\{X = x'\}$  is the probability that we obtain the events  $X = x'$ . By numerical method, we can evaluate this probability by

$$P\{X = x'\} = \frac{N\{X = x'\}}{\sum N\{\Omega\}}, \quad (36)$$

where  $\sum N\{\Omega\}$  is the total event number and  $N\{X = x'\}$  is the number of events whose final penetrating distance is  $x'$ . If  $x > 0$ , it is equivalent to transform to the other form,

$$\langle X \rangle = \sum_{x'} x' P\{X = x'\} = \int_0^{\infty} P\{X > x'\} dx'. \quad (37)$$

It is easy to prove that by considering the discrete system,  $dx = \Delta x = 1$ . We can rewrite the integral as

$$\begin{aligned} \int_0^{\infty} P\{X > x'\} dx' &= \sum_{x'=0}^{\infty} P\{X > x'\} \Delta x \\ &= \sum_{x'=0}^{\infty} P\{X > x'\} \\ &= P\{X = 1\} + P\{X = 2\} + P\{X = 3\} + \dots \\ &\quad + P\{X = 2\} + P\{X = 3\} + P\{X = 4\} + \dots \\ &\quad + P\{X = 3\} + P\{X = 4\} + P\{X = 5\} + \dots \\ &= 1 \cdot P\{X = 1\} + 2 \cdot P\{X = 2\} + 3 \cdot P\{X = 3\} + \dots \end{aligned}$$

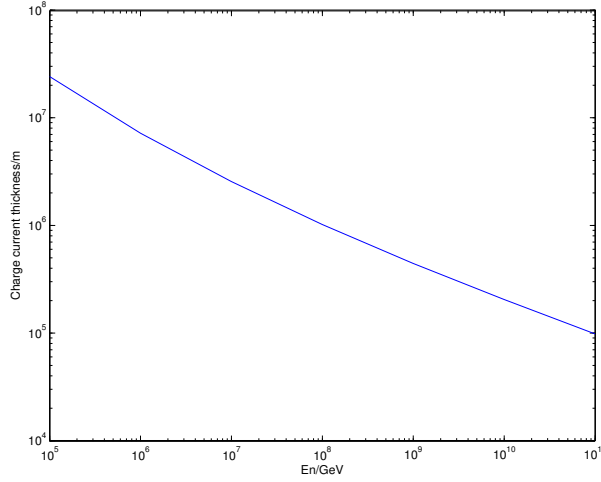


Figure 1: Charge current scattering thickness in standard rock.

$$= \sum_{x'} x' P\{X = x'\}.$$

### 3 Process for $\nu_\tau$ and $\tau$

We generate a process is that a million of  $\nu_\tau$  pass through the standard rock. Some  $\nu_\tau$  may lose their energy in rock, while a part of the  $\nu_\tau$  may change to  $\tau$  by the charge-current scattering, with the  $\nu_\tau \rightarrow \tau$  conversion rate depending on the  $\nu_\tau$  energy. After the charge-current scattering,  $\tau$  is produced and travels through the rock. Due to its interaction with the rock, the  $\tau$  energy is decreased. As a result,  $\tau$  may decay back to  $\nu_\tau$  and repeat the above process. Eventually, some of the  $\tau$  could come out of the rock and can be observed by the detector.

#### 3.1 Process for $\nu_\tau$

The neutral-current interaction takes away the energy of  $\nu_\tau$ , and the charge-current scattering changes  $\nu_\tau$  to  $\tau$ . The thickness of charge-current interaction is decreased with energy, as shown in Fig. 1 [4].

### 3.2 Process for $\tau$

As discussed in the previous section  $\tau$  is produced from the  $\nu_\tau$  charge-current scattering process. It may further go through the pair production [6] and photonuclear scatterings [7]. As a result,  $\tau$  loses its energy. Besides losing the energy,  $\tau$  may decay to  $\nu_\tau$  by the following processes [2],

$$\tau \rightarrow \nu_\tau \mu \nu_\mu, \quad (38)$$

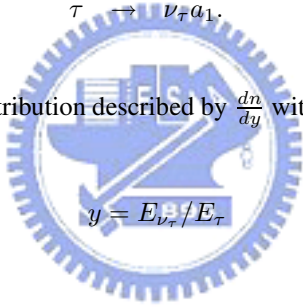
$$\tau \rightarrow \nu_\tau e \nu_e, \quad (39)$$

$$\tau \rightarrow \nu_\tau \pi, \quad (40)$$

$$\tau \rightarrow \nu_\tau \rho, \quad (41)$$

$$\tau \rightarrow \nu_\tau a_1. \quad (42)$$

where the  $\nu_\tau$  energy is a distribution described by  $\frac{dn}{dy}$  with

$$y = E_{\nu_\tau} / E_\tau \quad (43)$$


The energy of  $\nu_\tau$  is

$$E_{\nu_\tau} = y E_\tau. \quad (44)$$

As in the previous section,  $y$  is calculated by a random number  $r$  with Eq. (12). Fig. 2 shows the distribution of  $y$ . Only the range of process (38) is  $[0, 1]$ . The range of  $y$  for each decay channel is shown in Table 1. We note that  $\nu_\tau$  can also be produced from  $\tau$  by the charge-current scattering.



Process	$y_{min}$	$y_{max}$	Branching ratio
$\tau \rightarrow \nu_\tau \mu \nu_\mu$	0	1	0.18
$\tau \rightarrow \nu_\tau e \nu_e$	0	1	0.18
$\tau \rightarrow \nu_\tau \pi$	0	0.9938	0.12
$\tau \rightarrow \nu_\tau \rho$	0	0.8130	0.26
$\tau \rightarrow \nu_\tau a_1$	0	0.5209	0.13

Table 1: The range of  $y$  for the  $\tau$  decay processes.

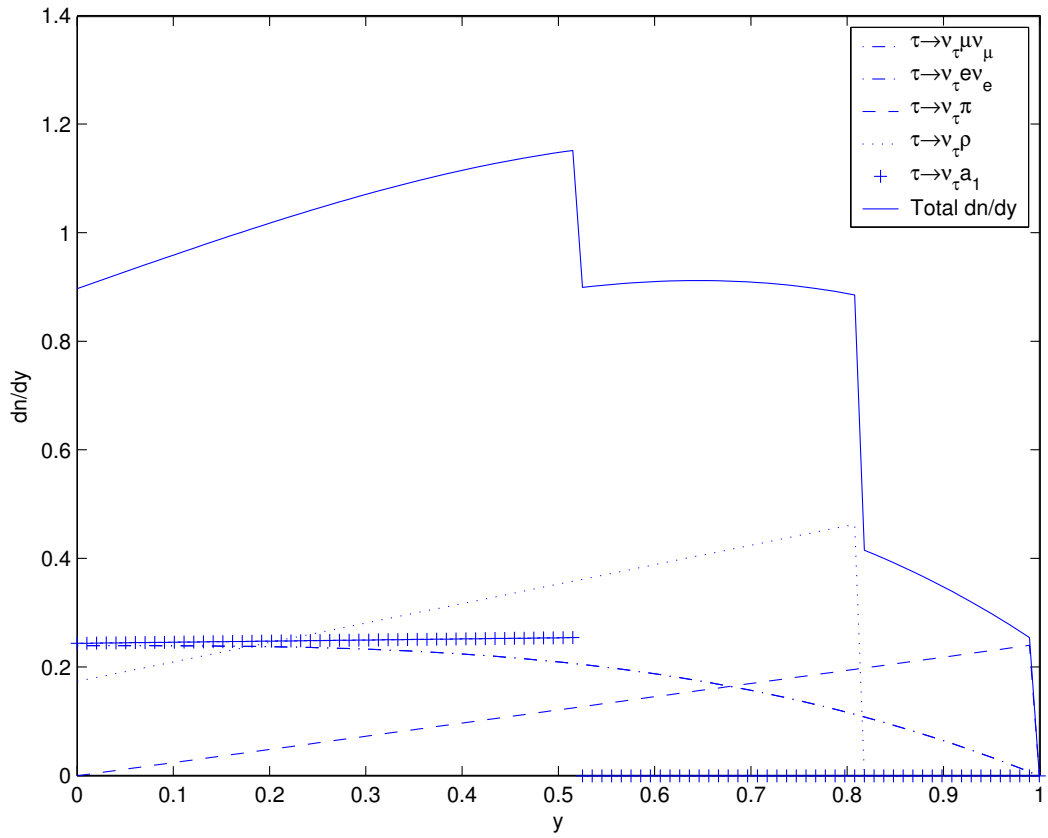


Figure 2: The distribution of  $y$  for the  $\tau$  decay processes.

## 4 Tau-lepton energy loss

### 4.1 Deterministic approach

If we assume that the scattering process is deterministic, the energy loss,

$$-dE \equiv \langle y \rangle E dP_\sigma, \quad (45)$$

is also deterministic, where  $\langle y \rangle$  is the expectation value of  $y$ , which is defined in Eq. (19) and  $dP_\sigma$  is the tau-lepton interaction probability,

$$dP_\sigma = \frac{dx}{L}, \quad (46)$$

with  $L$  the interaction thickness. The interaction thickness can be calculated by

$$L = \frac{1}{n\sigma}, \quad (47)$$

where  $\sigma$  is the tau-lepton interaction cross section and  $n$  is the number density of the medium nuclei,

$$n = \frac{\rho N_A}{A}, \quad (48)$$

with  $\rho$  the medium density,  $N_A$  the Avogadro's number,  $A$  the mass of target nucleus per mole. From Eq. (45) :

$$\begin{aligned} -dE &= \langle y \rangle E dP_\sigma \\ &= \langle y \rangle E \frac{dx}{L} \\ &= \langle y \rangle E \frac{\rho N_A}{A} \sigma dx \\ &= E \rho dx \frac{N_A}{A} \int_{y_{\min}}^{y_{\max}} y \frac{d\sigma}{dy} dy \\ &= \frac{N_A}{A} E dX \int_{y_{\min}}^{y_{\max}} y \frac{d\sigma}{dy} dy, \end{aligned} \quad (49)$$

where we have applied

$$\langle y \rangle = \frac{1}{\sigma} \int_{y_{\min}}^{y_{\max}} y \frac{d\sigma}{dy} dy$$

and

$$dX = \rho dx.$$

The energy loss per unit slant depth (in units of g/cm<sup>2</sup>) can be expressed in the form:

$$-\frac{dE}{dX} = \sum_i \beta_i E \quad (50)$$

$$X = \rho x, \quad (51)$$

where  $\rho$  is the medium density and  $x$  is the distance in cm,  $\beta_i$  is defined as

$$\beta_i = \frac{N}{A} \int_{y_{\min}}^{y_{\max}} y \frac{d\sigma_i}{dy'} dy'. \quad (52)$$

The  $i$  denotes the type of interactions. In other words, we consider all types of interactions, photonuclear and pair production, for the tau-lepton energy loss. In the deterministic approach, we take the average for the fraction of energy loss  $y$ . Hence  $\beta_i$  is an exact value, so is the  $\frac{dE}{dX}$ ,

$$-\frac{dE}{dX} = \sum_i \frac{NE}{A} \int_{y_{\min}}^{y_{\max}} y \frac{d\sigma_i}{dy} dy. \quad (53)$$

## 4.2 Stochastic approach

The previous section shows that the process is deterministic when we take the average for  $\beta_i$ . From Eq. (10), we can rewrite Eq. (52) into

$$\beta_i = \frac{N\sigma_i}{A} \int_{y_{\min}}^{y_{\max}} y \frac{dP}{dy} dy = \frac{N\sigma_i}{A} \langle y \rangle. \quad (54)$$

In this form,  $\beta_i$  is a function of total cross section  $\sigma_i$  and the expectation value of  $y$ . In Sec. 2.4, Monte-carlo method turns the problem from an integral to an average,

$$\beta_i = \frac{N\sigma_i}{A} \langle y \rangle \equiv \frac{N\sigma_i}{A} \sum_{j=1}^N \frac{y_j}{N}. \quad (55)$$

However, this is still not our goal because this  $\beta_i$  is still an average value for one step of energy loss. We intend to consider each event individually. The procedure is :

1. Calculate interaction thickness  $L$  by Eq. (47).
2. Choose the length for each step  $dx$ , such that the interaction probability  $dp$  for each step of tau-lepton propagation is  $dp = \frac{dx}{L}$ .
3. Generate a random number to determinate whether or not the interaction occurs. The probability must be equal to  $dp$  we have before.
4. If the interaction happens, the energy loss should be  $y \cdot E$  for the distance  $dx$ .

We remark that, in step 2,  $dx$  is decreased with  $dx$ . Does the energy loss depend on the choice for  $dx$ ? To make sure, we compare the total energy loss for two different  $dx$  case. If we choose  $(dx)_1 = 0.1 \cdot L$  and  $(dx)_2 = 0.01 \cdot L$ ,  $dp_1 = 0.1$  and  $dp_2 = 0.01$ . For the total interval  $h$ , the first case performs  $10 \frac{h}{L}$  times energy loss processes and  $100 \frac{h}{L}$  times for the second one. It is important to recall that the chance for an energy loss to occur, is  $p_1 = 0.1$  for the first case and  $p_2 = 0.01$  for the second case. Thus, it is harder for the second case to interact. Consequently, the choice of interaction probability does not effect the total energy loss if we neglect the other numerical problems.

#### 4.2.1 Hard-term energy loss

Knowing that the tau-lepton energy loss can be deduced from a random variable, we proceed to discuss the hard term energy loss. In order to evaluate the energy loss from Sec. 4.2, we need to obtain a  $y_j$  from a random number mapping, shown as Sec. 2.3 shows. Thus, we integrate the differential cross section over the interval  $[y_{\min}, y]$ ,

$$r = \frac{1}{\sigma} \int_{y_{\min}}^y \frac{d\sigma}{dy'} dy'. \quad (56)$$

However,  $\frac{d\sigma}{dy}$  [5] has a singular point at  $y = 0$ . Hence the integral diverges as  $y \rightarrow 0$ . We set  $y_{\text{cut}} > y_{\text{min}}$  in order to avoid this problem,

$$r = \frac{1}{\sigma} \int_{y_{\text{cut}}}^y \frac{d\sigma}{dy'} dy'. \quad (57)$$

When we pick up a  $y$  from this integral, the energy loss is called the hard-term. The remaining energy loss in the region  $[y_{\text{min}}, y_{\text{max}}]$ ,  $[y_{\text{min}}, y_{\text{cut}}]$ , is compensated by the soft-term in Sec. 4.2.2.

#### 4.2.2 Soft-term energy loss

Since the integral region of  $y$  is reduced from  $[y_{\text{min}}, y_{\text{max}}]$  to  $[y_{\text{cut}}, y_{\text{max}}]$  in the hard-term energy loss, it is essential to restore the energy loss from  $[y_{\text{min}}, y_{\text{cut}}]$ . We treat this term as a deterministic process. From Eq. (53),

$$-\left(\frac{dE}{dX}\right)_{\text{soft}} = \sum_i \frac{NE}{A} \int_{y_{\text{min}}}^{y_{\text{cut}}} y \frac{d\sigma_i}{dy} dy. \quad (58)$$

This energy loss term is called the soft-term. The integral of  $y \frac{d\sigma_i}{dy}$  on  $[y_{\text{min}}, y_{\text{cut}}]$  is finite due to  $y \rightarrow 0$ . Furthermore, the whole energy loss is the sum of soft and hard term,

$$-\frac{dE}{dX} = \sum_i E \left( \frac{N}{A} \int_{y_{\text{min}}}^{y_{\text{cut}}} y \frac{d\sigma_i}{dy} dy + y_j \right). \quad (59)$$

The  $i$  denotes the type of the interaction and  $y_j$  the random variable. Remark that only the hard term,  $E \cdot y_j$ , is treated as a stochastic process.

## 5 Simulation results

First, we start from the propagation of tau-lepton inside the standard rock. In this situation, we only need to consider the pair production and photonuclear interactions which cause the energy loss of  $\tau$ . In view of experimental situation, we require the simulation to stop at  $E_\tau = 50$  GeV [1]. We consider a system that the medium is unlimited in order to measure the penetrating distance of incident  $\tau$ , and consequently determine

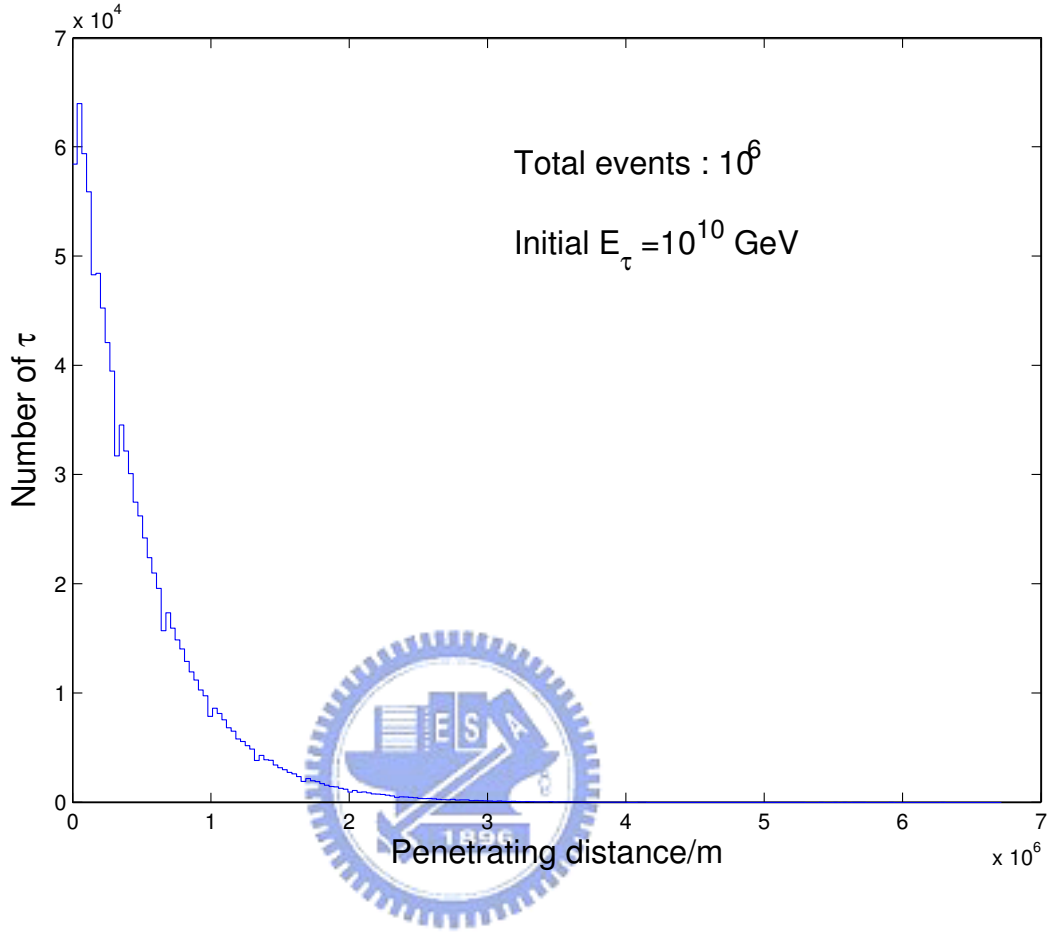


Figure 3: The tau-lepton penetrating distance in the standard rock considering only decay (without energy loss interaction). Initial tau-lepton energy is  $10^{10}$  GeV. The exponential decay constant is about  $-2 \times 10^{-6}/\text{m}$ .

the  $\tau$  range. This algorithm has been shown in Sec. 2.9. By simulating the incident tau-leptons, we can obtain the  $\tau$  range by Eq. (35) and Eq. (36). It is the expectation value of tau-lepton penetrating distance in the medium. The tau-lepton ranges from the Monte-carlo method are compared with the deterministic results. They are shown in Fig. 4, 6, 9 and the fractions of difference between two approaches are illustrated in Fig. 7,11. The comparison of our result with other Monte-carlo calculation [1], is shown in Fig. 10.

Having obtained the tau-lepton range, we consider the  $\nu_\tau$  process with a finite medium length. In the  $\nu_\tau$  process, incident  $\nu_\tau$  may change to  $\tau$  after the charge-current

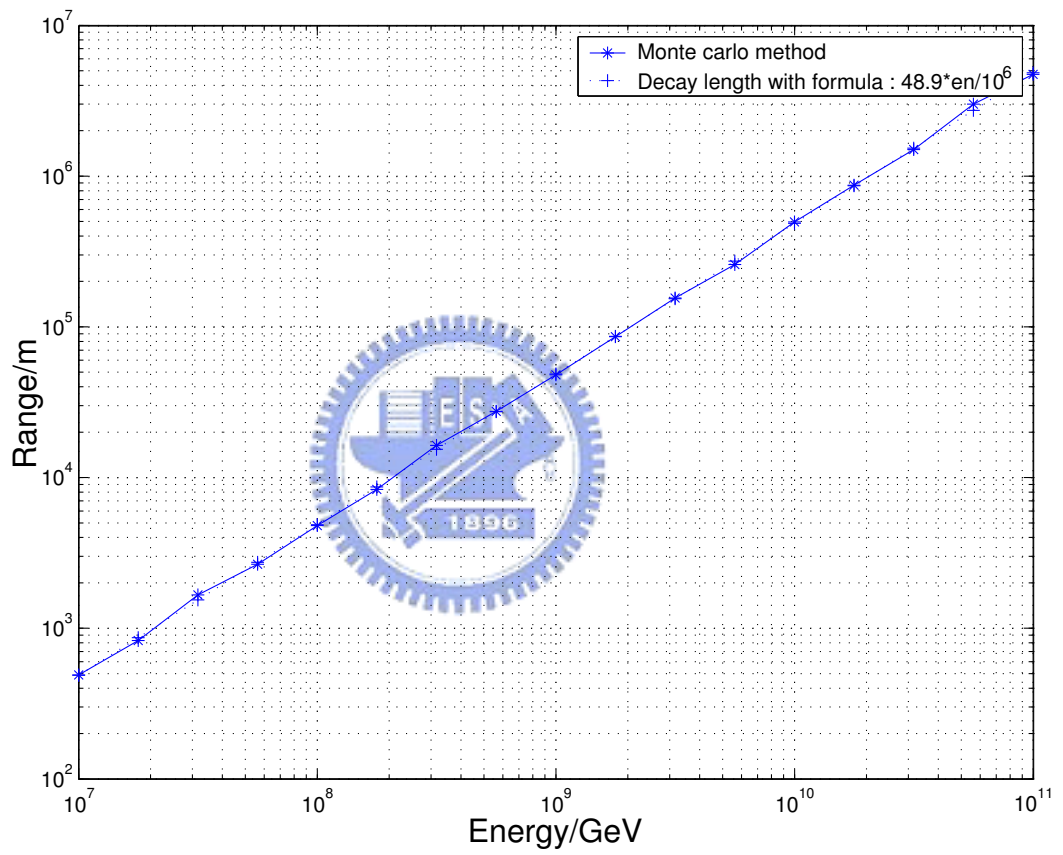


Figure 4: Tau-lepton range considering only the decay process.

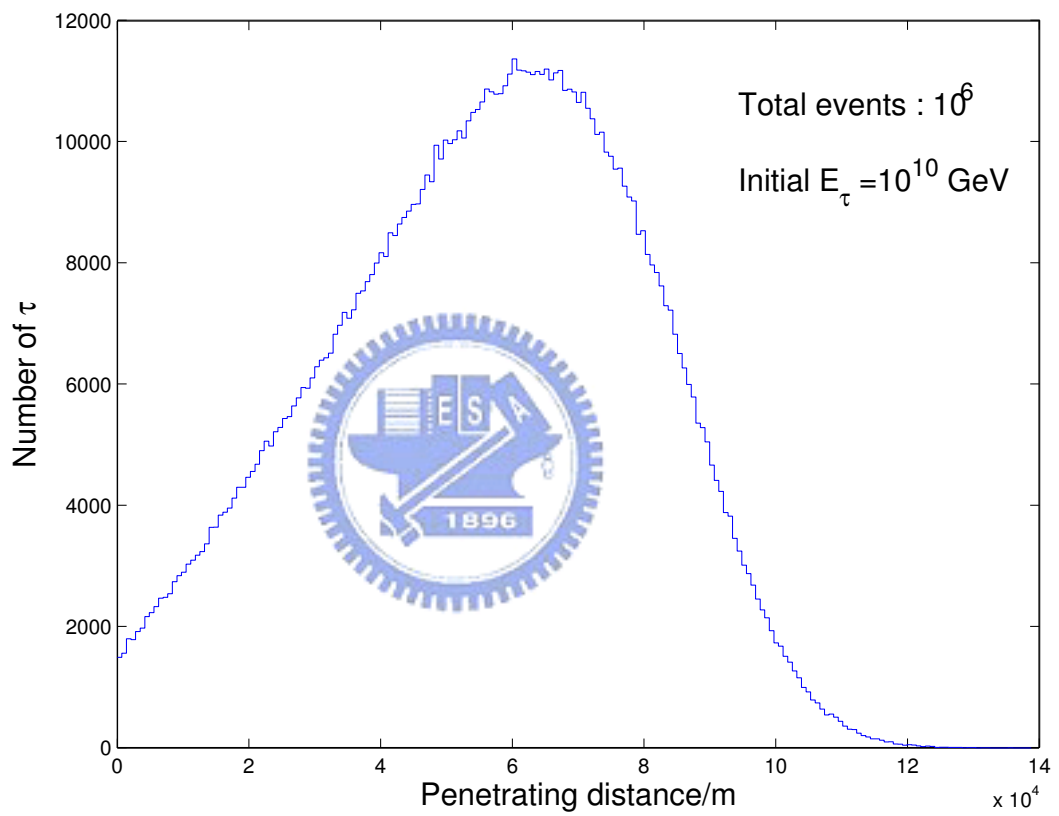


Figure 5: The tau-lepton penetrating distance inside the standard rock considering the pair production interaction. Initial energy of  $\tau$  is  $10^{10}$  GeV.



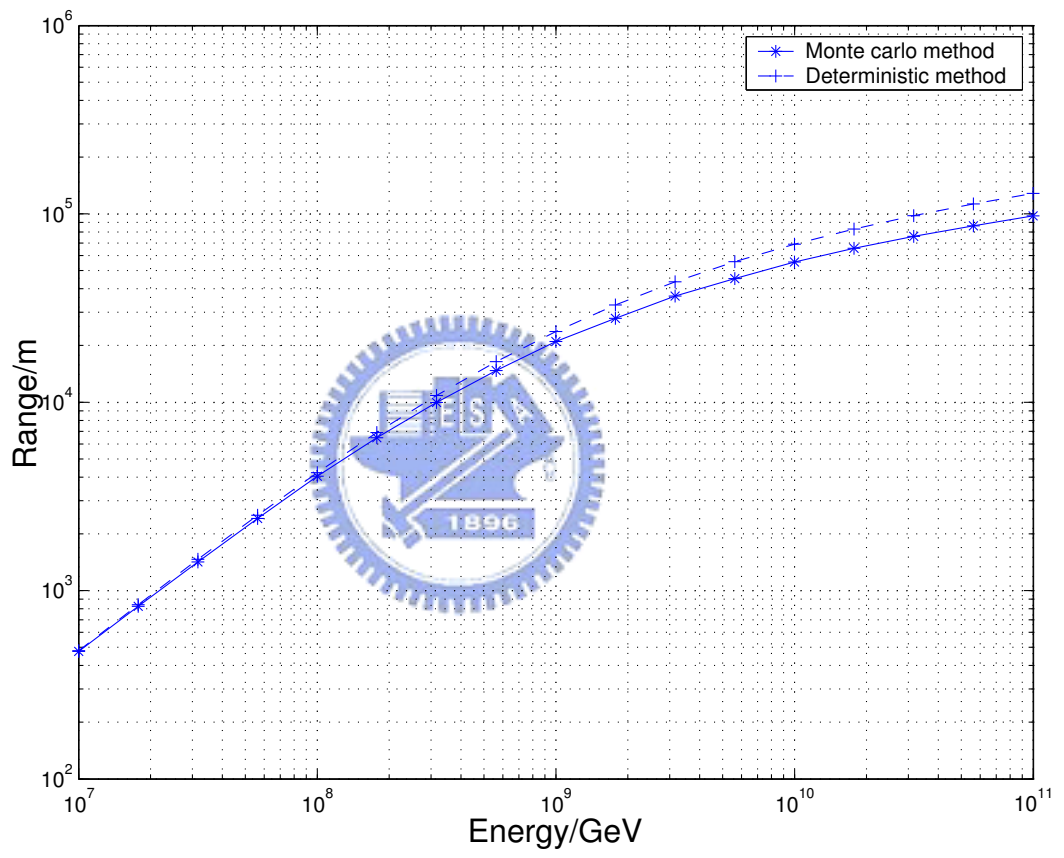


Figure 6: Tau-lepton range considering the pair production interaction.

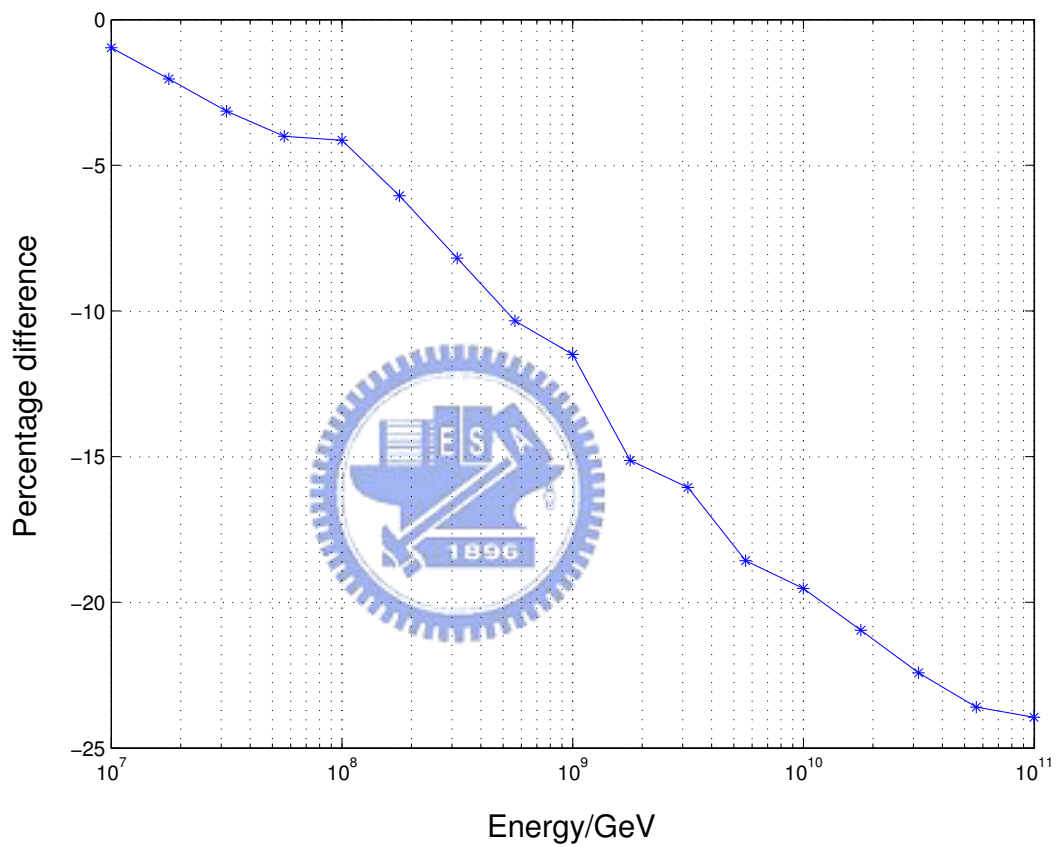


Figure 7: The fraction of difference in the tau-range between the Monte-carlo method and the deterministic method. The comparison is made by considering only the pair-production loss.

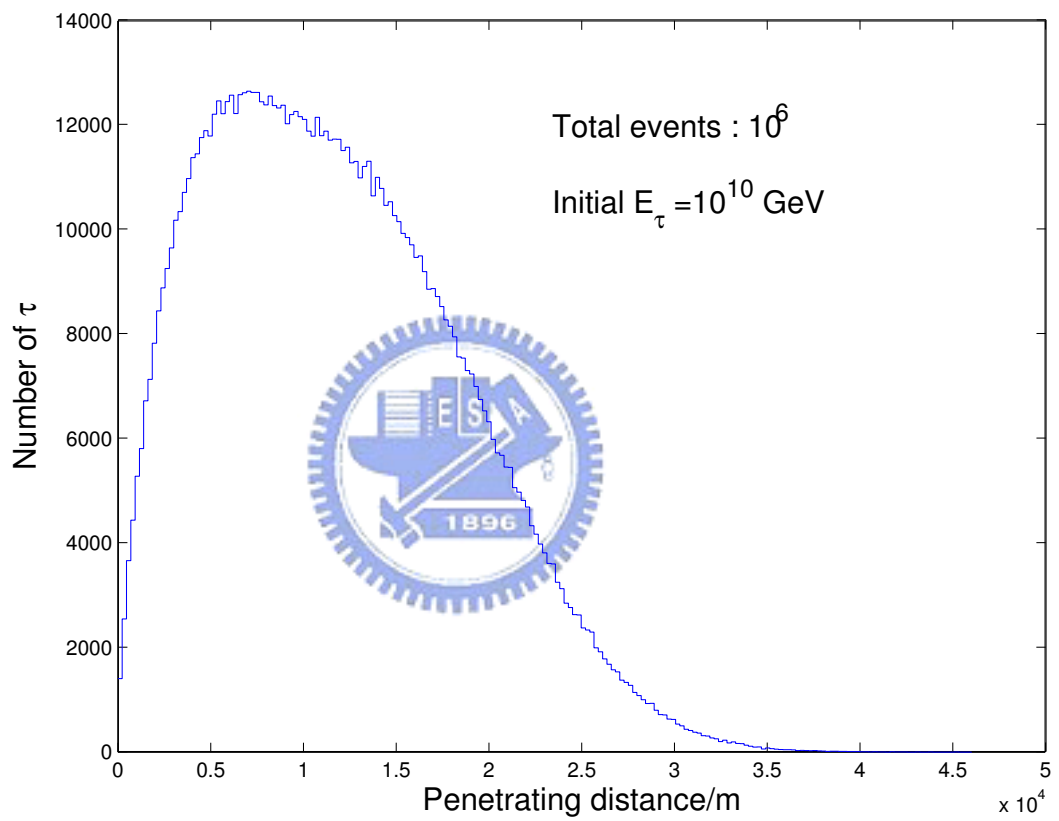


Figure 8: The tau-lepton penetrating distance inside the standard rock considering the pair production and photonuclear interactions. Initial energy of  $\tau$  is  $10^{10}$  GeV.

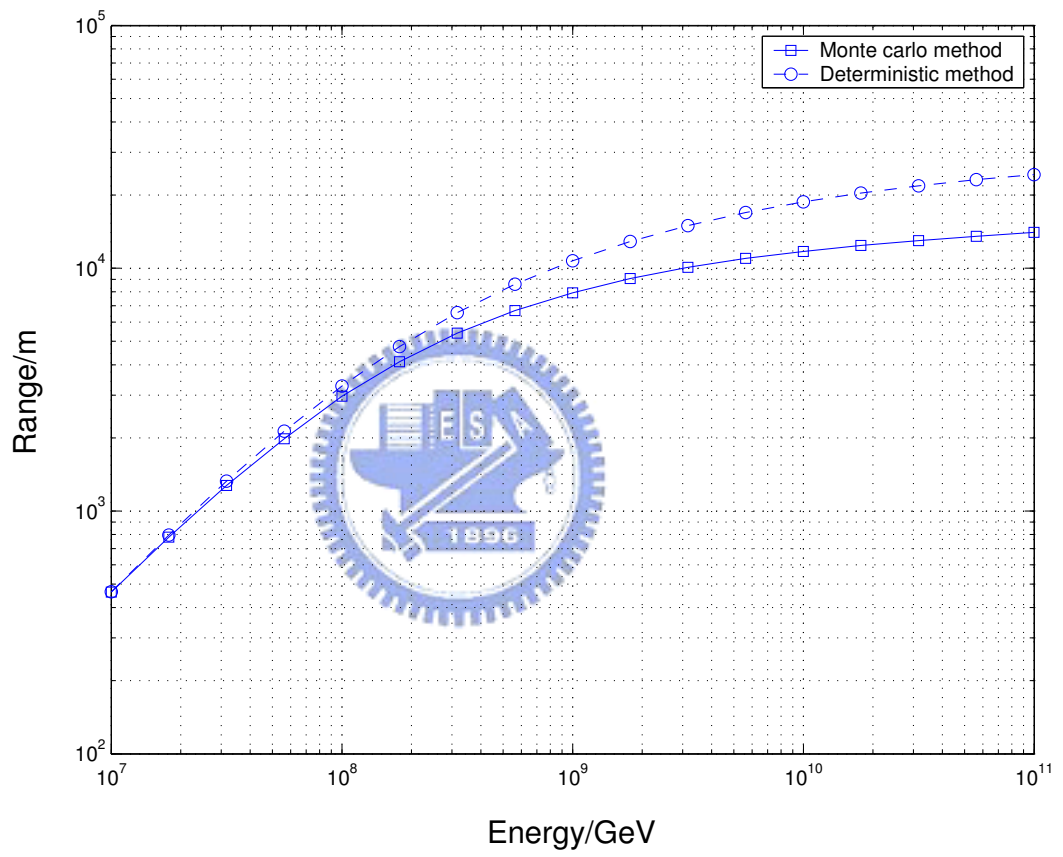


Figure 9: Tau-lepton range considering the pair production and photonuclear interactions.

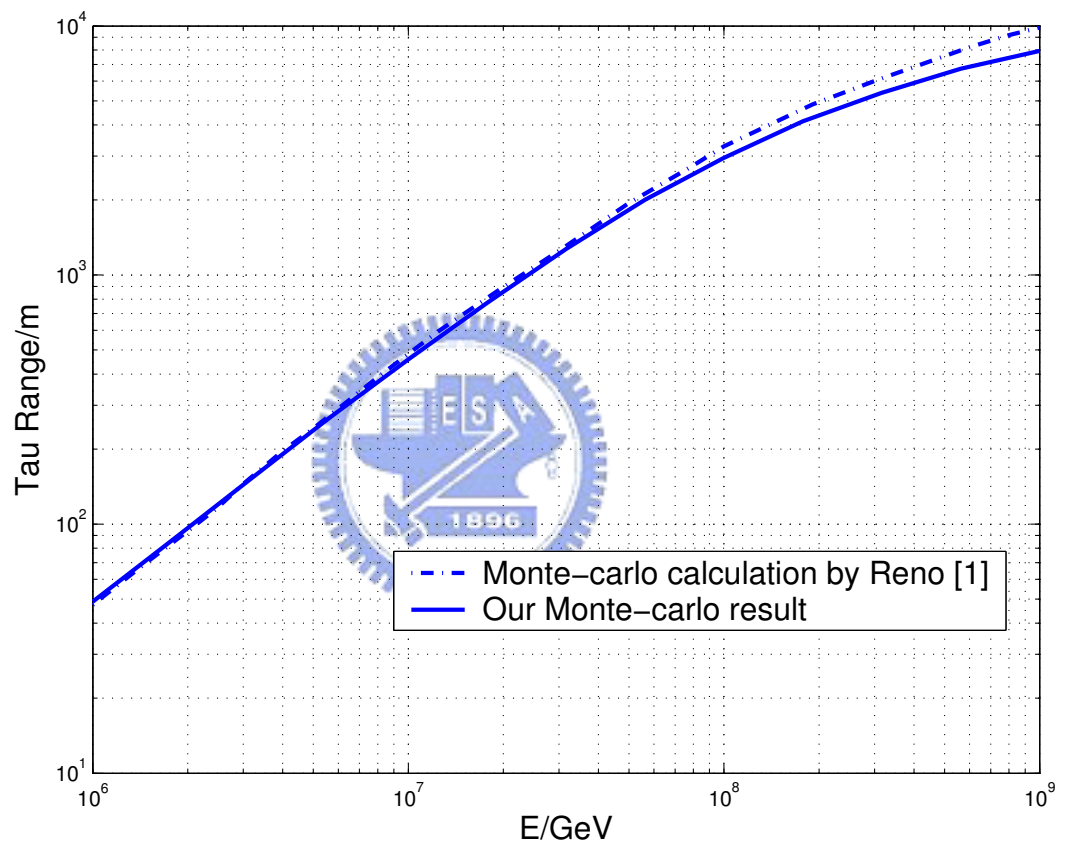


Figure 10: The comparison with the Monte-carlo calculation by Reno [1].

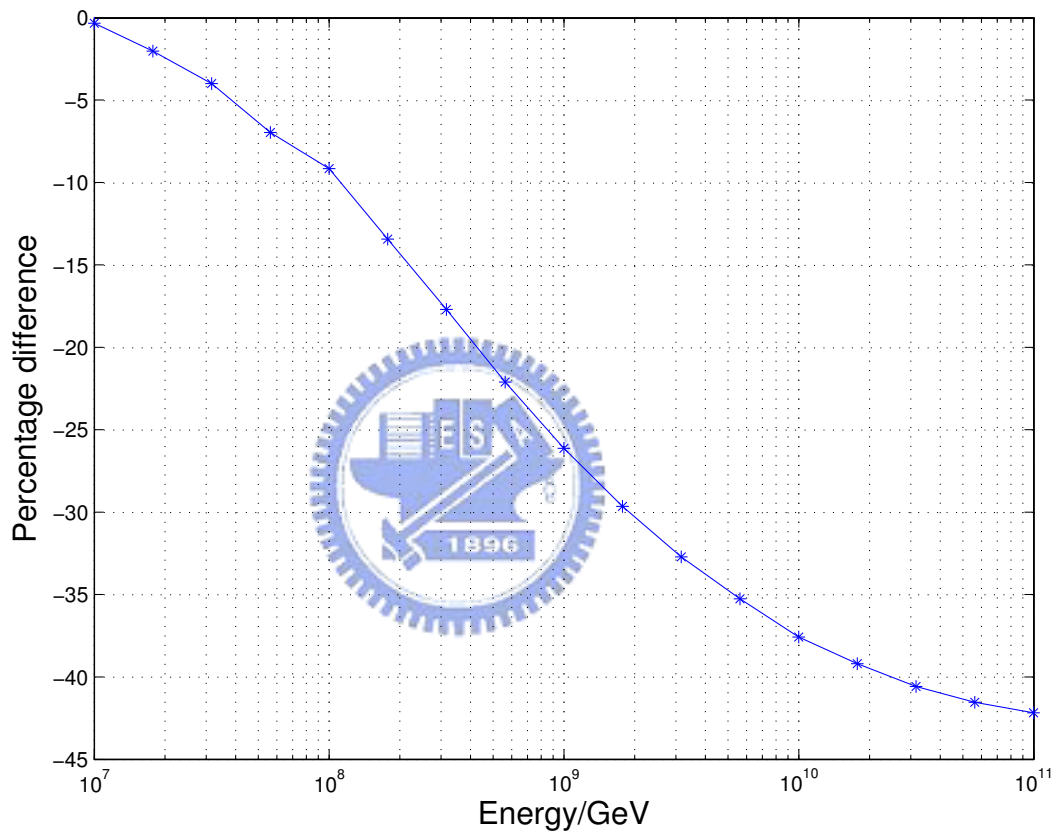


Figure 11: The fraction of difference in the tau-range between the Monte-carlo method and the deterministic method. The comparison is made by considering the pair-production and photonuclear losses.

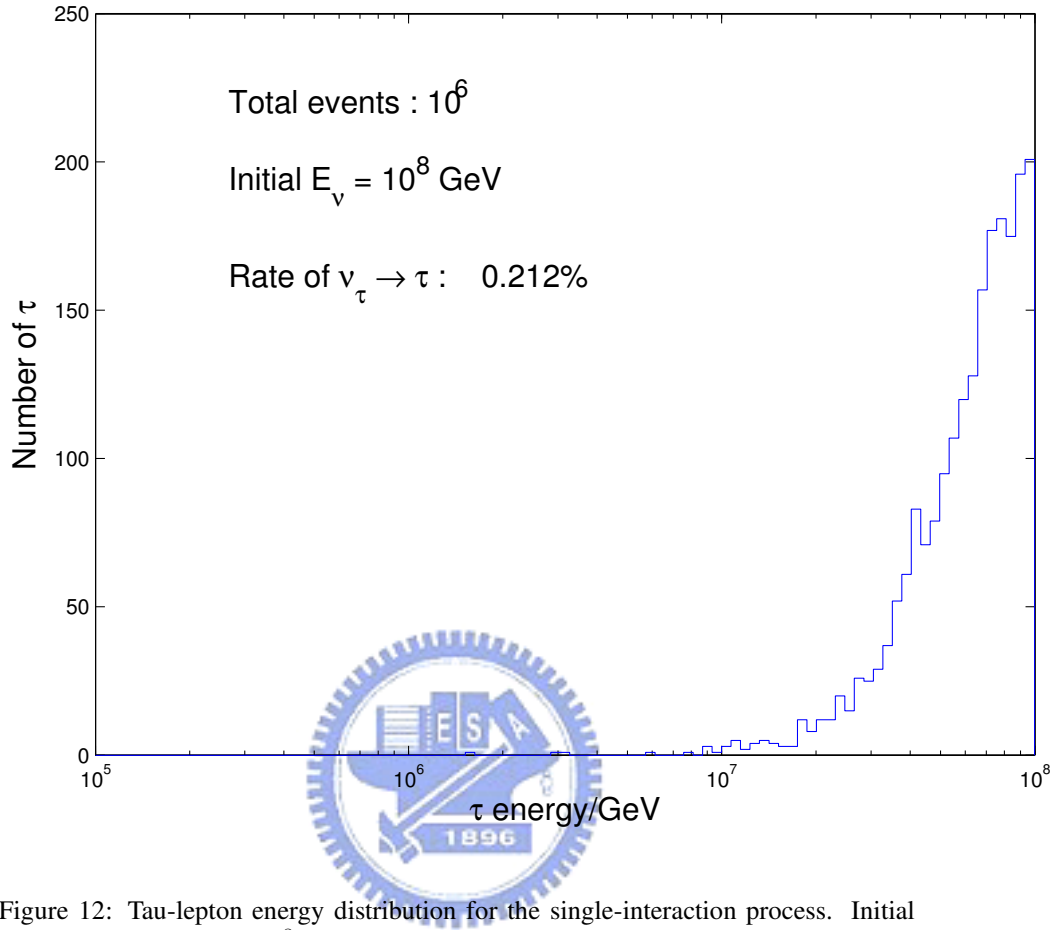


Figure 12: Tau-lepton energy distribution for the single-interaction process. Initial energy of incident  $\nu_\tau$  is  $10^8$  GeV.

scattering. Then only some of the  $\tau$  can travel to the end of medium without decaying. We shall calculate the energy distribution of these survival  $\tau$ . We simulate the incident  $\nu_\tau$  propagating into three different medium lengths,  $2 \times 10^4$ ,  $5 \times 10^4$ ,  $10^5$  m standard rock. A detector is placed at some distance from the end of the medium to count the number of survival  $\tau$ . This is the way to detect  $\nu_\tau$  in the neutrino-telescope experiment. The energy distributions for  $\tau$  and the conversion rate for  $\nu_\tau \rightarrow \tau$  are shown in Fig. 12, 13, 14 show.

In addition, the multiple interaction is possible if we consider the decay process and charge-current scattering of  $\tau$ . This outgoing  $\nu_\tau$  is a new source of input for the system. But the energy of this type of regenerated  $\nu_\tau$  is lower than the original due to the large energy loss of  $\tau$  interactions. The simulation is restarted with lower energy

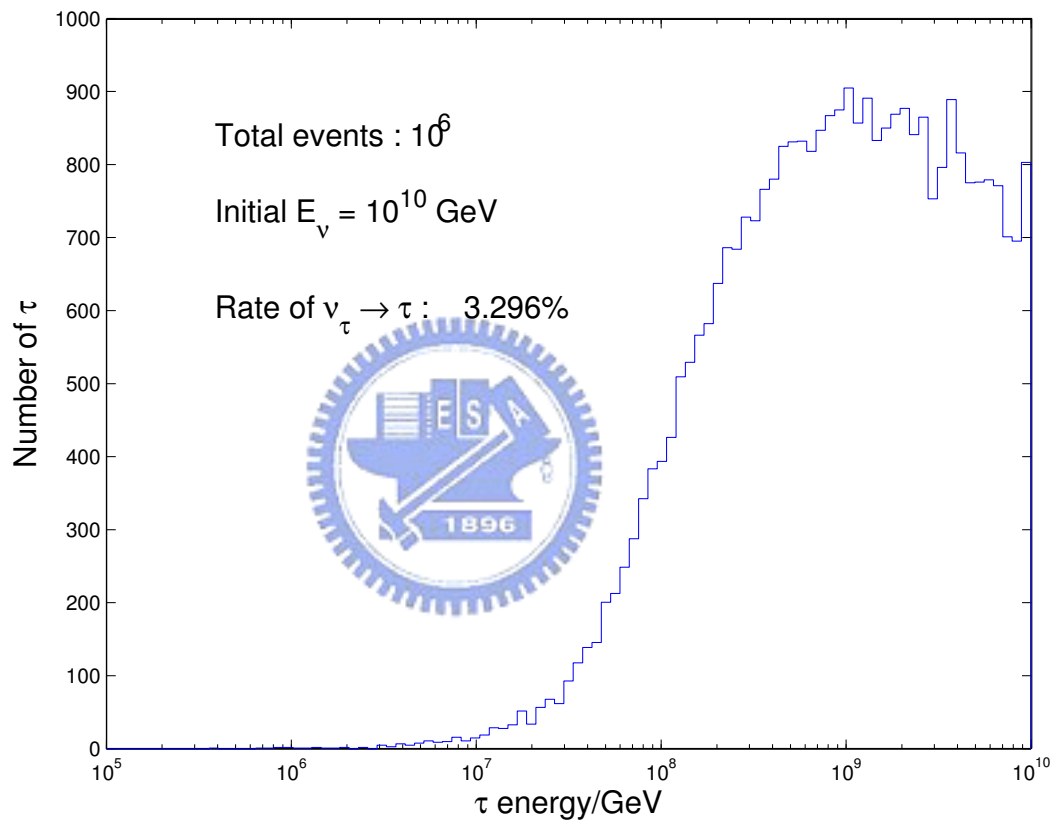


Figure 13: Tau-lepton energy distribution for the single-interaction process. Initial energy of incident  $\nu_\tau$  is  $10^{10}$  GeV.



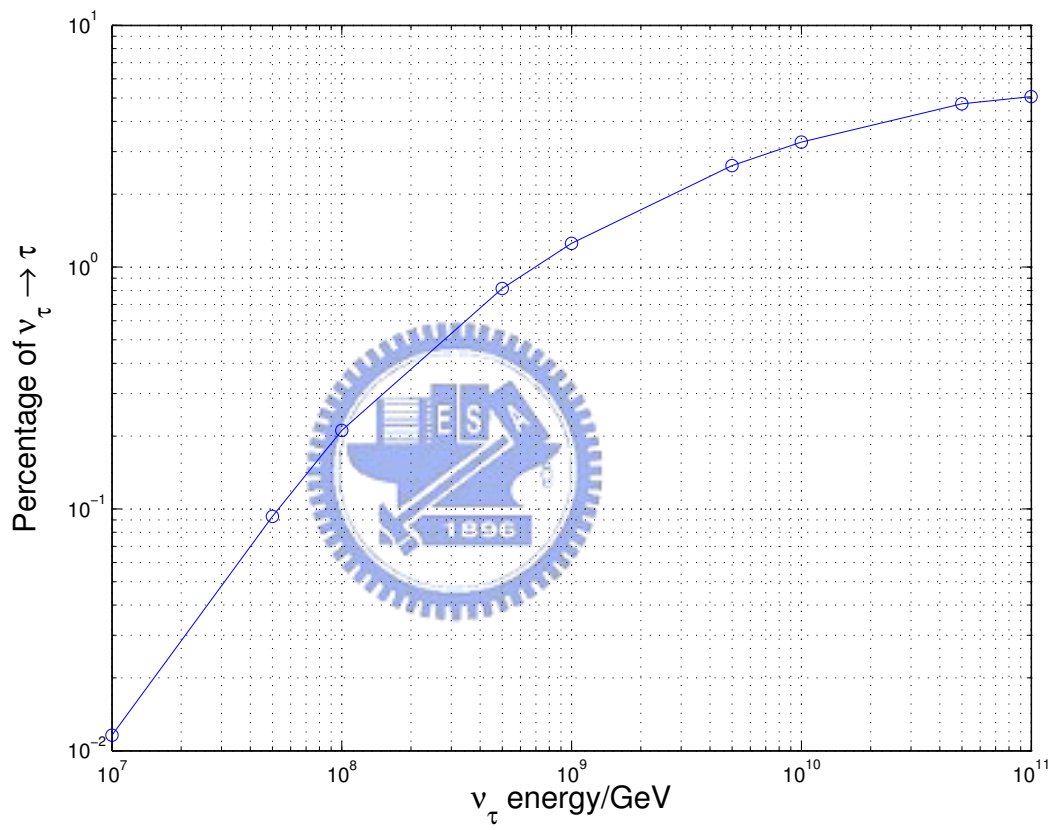


Figure 14: The conversion percentage for  $\nu_\tau \rightarrow \tau$  in a single-interaction process with the medium length  $10^5$  m.

incident  $\nu_\tau$ . Although the interaction thickness of charge-current is increased, some extra events may convert into  $\tau$  and received by the detector. Fig. 15-23 show the energy distribution.



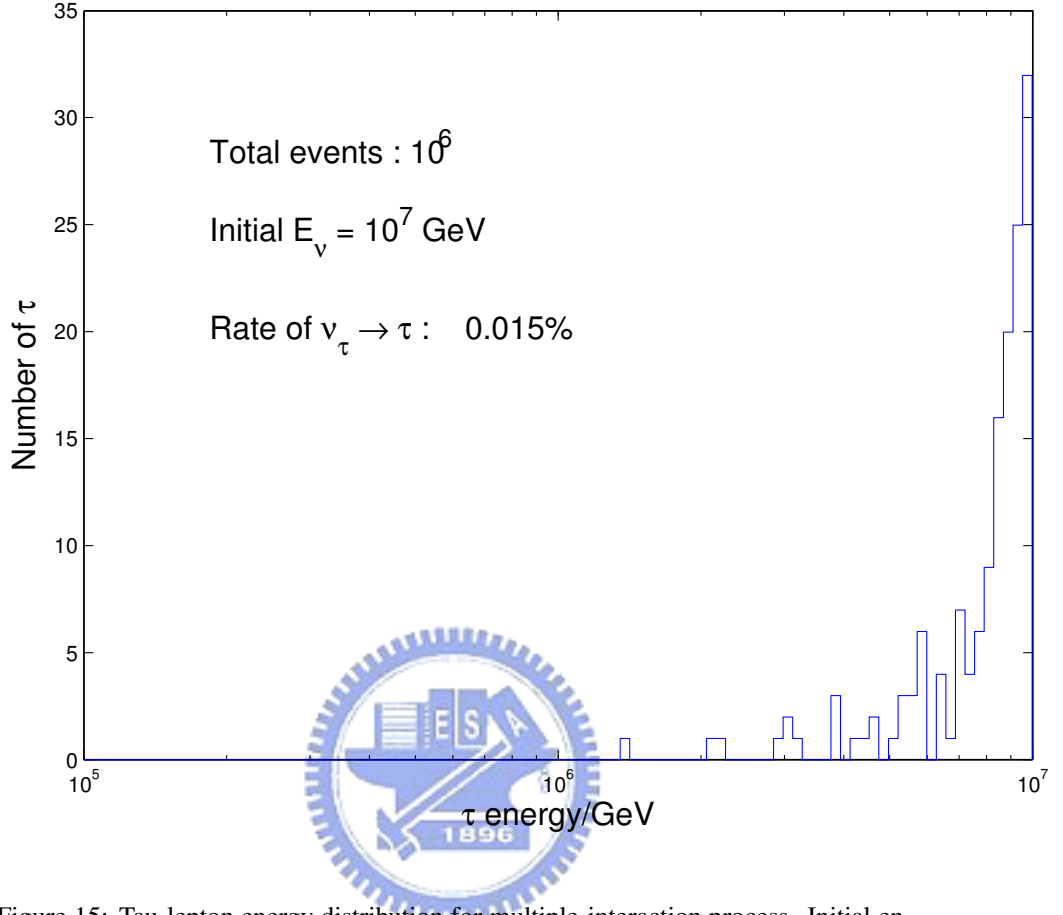


Figure 15: Tau-lepton energy distribution for multiple-interaction process. Initial energy of incident  $\nu_\tau$  is  $10^7$  GeV and the thickness of standard rock is  $2 \times 10^4$  m.

## 6 Discussion

In the unbounded medium case, we calculate the tau range, which is the average tau-lepton penetrating distance in the medium. The range for  $10^{10}$  GeV tau-lepton without energy loss is  $5 \times 10^5$  m, shown as Fig. 4. But the range is decreased to  $5.5 \times 10^4$  m when we consider the pair production energy loss, shown as Fig. 6. Furthermore, the range is  $1.2 \times 10^4$  m after adding the photonuclear energy loss. Thus, the tau range is decreased by the scatterings. In addition, we obtain a distribution of tau-lepton penetrating distance rather than an average value, Fig. 3, 5, 8, by the Monte-carlo method. When comparing results of the Monte-carlo method with those given by the deterministic method [3], we find that the tau range in Monte-carlo method is shorter.

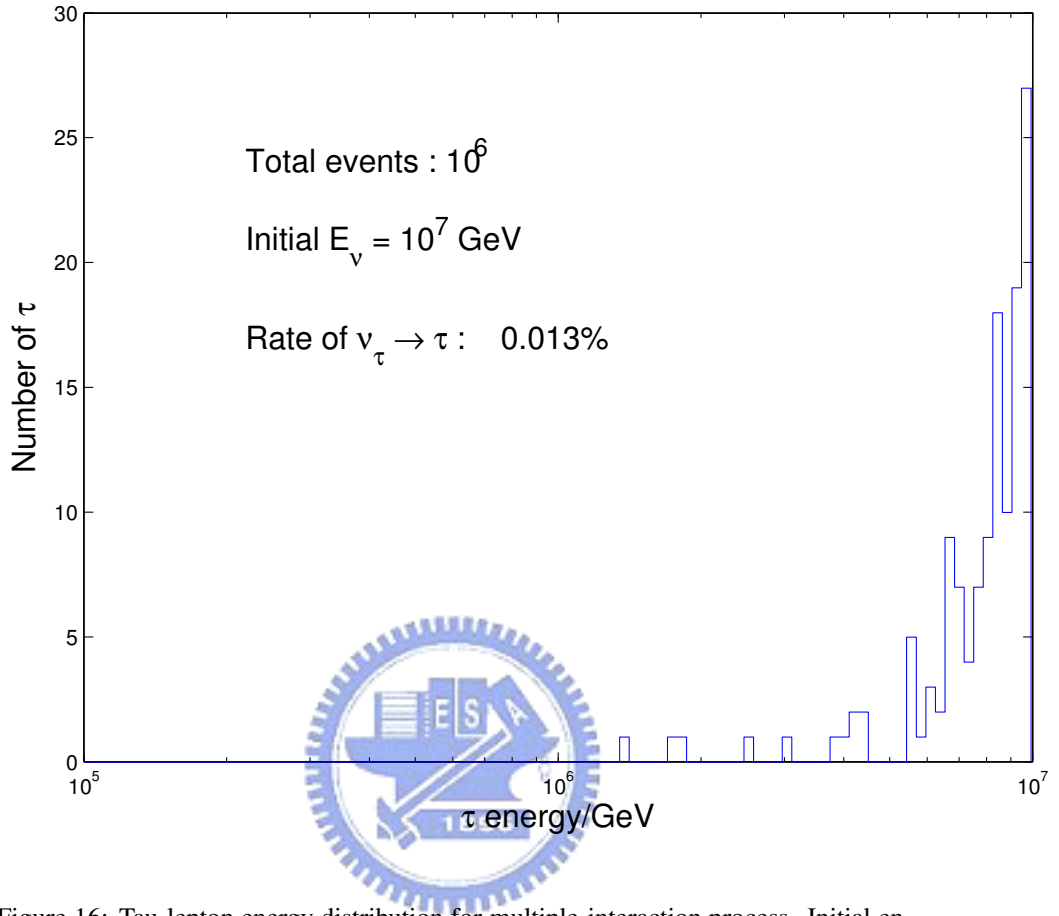


Figure 16: Tau-lepton energy distribution for multiple-interaction process. Initial energy of incident  $\nu_\tau$  is  $10^7$  GeV and the thickness of standard rock is  $5 \times 10^4$  m.

Rock thickness	$\nu_\tau \rightarrow \tau$ rate
$2 \times 10^4$ m	0.015%
$5 \times 10^4$ m	0.013%
$1 \times 10^5$ m	0.013%

Table 2: The relation between standard rock thickness and  $\nu_\tau \rightarrow \tau$  rate for  $E_\nu = 10^7$  GeV.

Rock thickness	$\nu_\tau \rightarrow \tau$ rate
$2 \times 10^4$ m	4.8%
$5 \times 10^4$ m	4.307%
$1 \times 10^5$ m	3.385%

Table 3: The relation between standard rock thickness and  $\nu_\tau \rightarrow \tau$  rate for  $E_\nu = 10^{10}$  GeV.

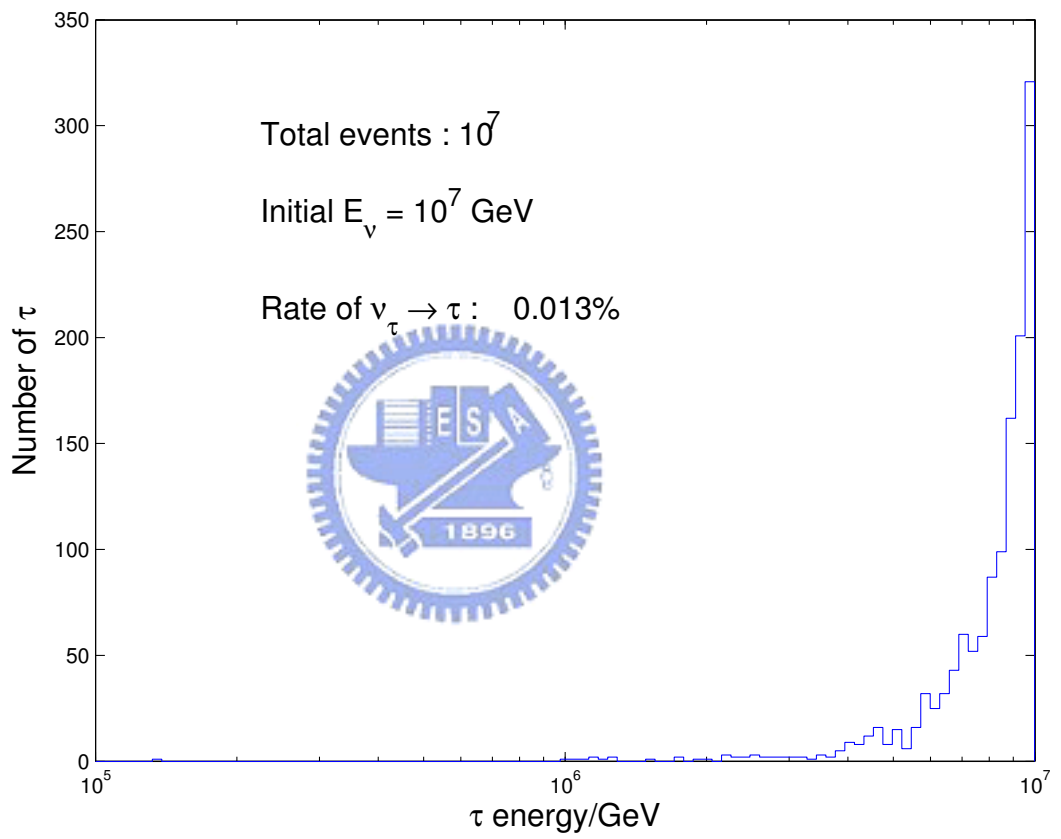


Figure 17: Tau-lepton energy distribution for multiple-interaction process. Initial energy of incident  $\nu_\tau$  is  $10^7$  GeV and the thickness of standard rock is  $1 \times 10^5$  m.

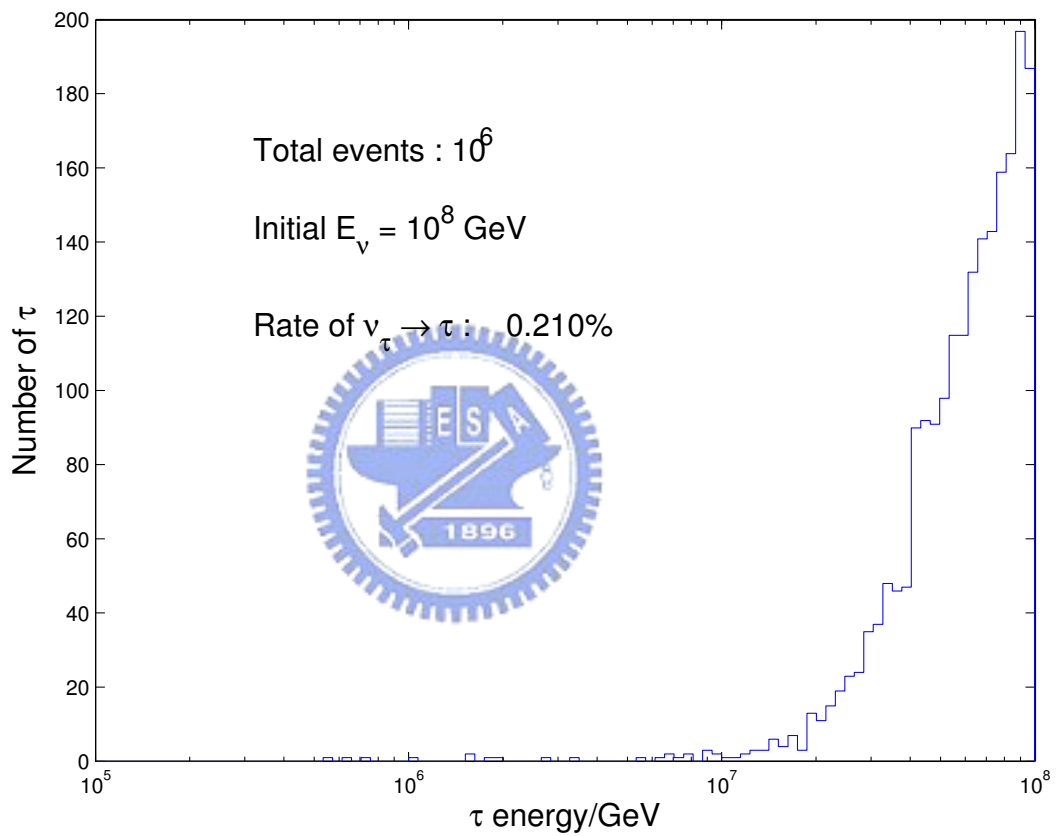


Figure 18: Tau-lepton energy distribution for multiple-interaction process. Initial energy of incident  $\nu_\tau$  is  $10^8$  GeV and the thickness of standard rock is  $1 \times 10^5$  m.

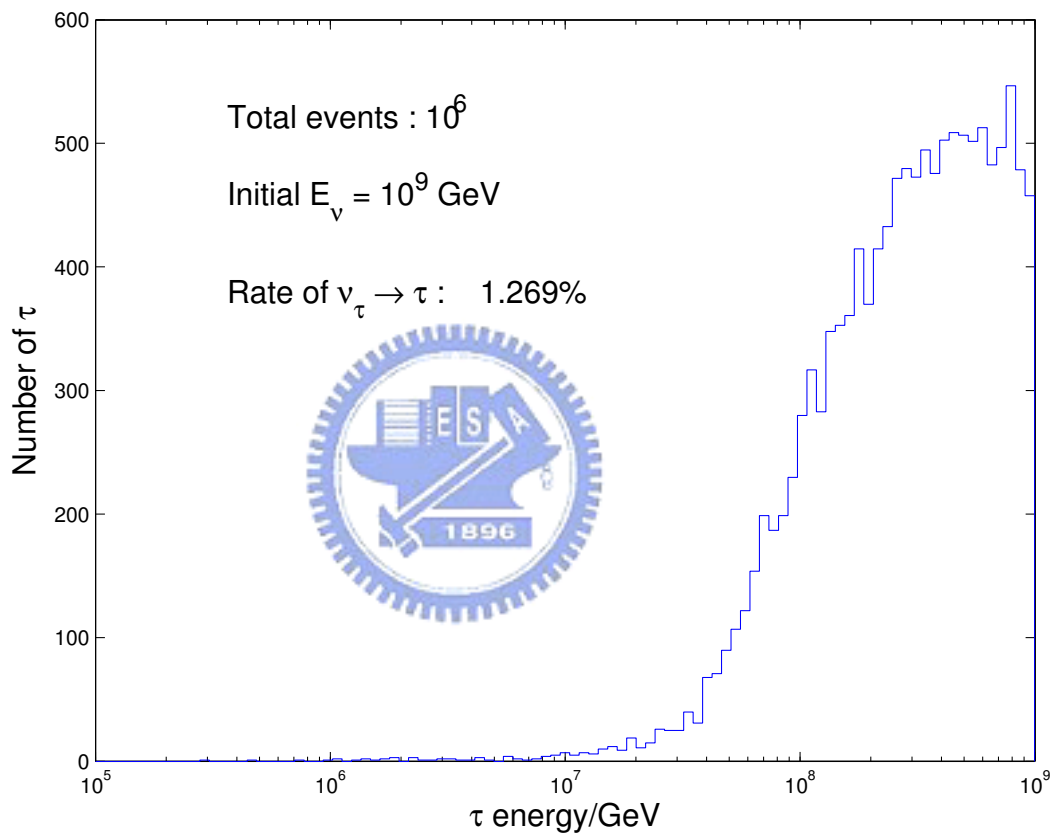


Figure 19: Tau-lepton energy distribution for multiple-interaction process. Initial energy of incident  $\nu_\tau$  is  $10^9$  GeV and the thickness of standard rock is  $1 \times 10^5$  m.

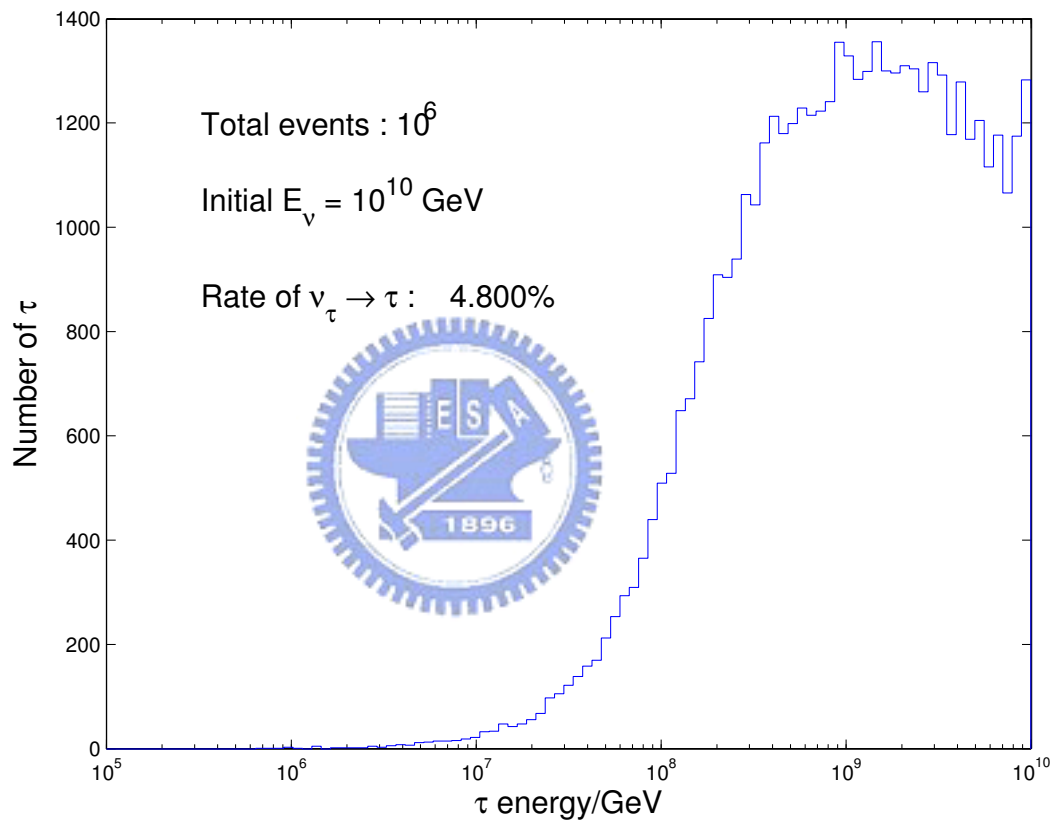


Figure 20: Tau-lepton energy distribution for multiple-interaction process. Initial energy of incident  $\nu_\tau$  is  $10^{10}$  GeV and the thickness of standard rock is  $2 \times 10^4$  m.



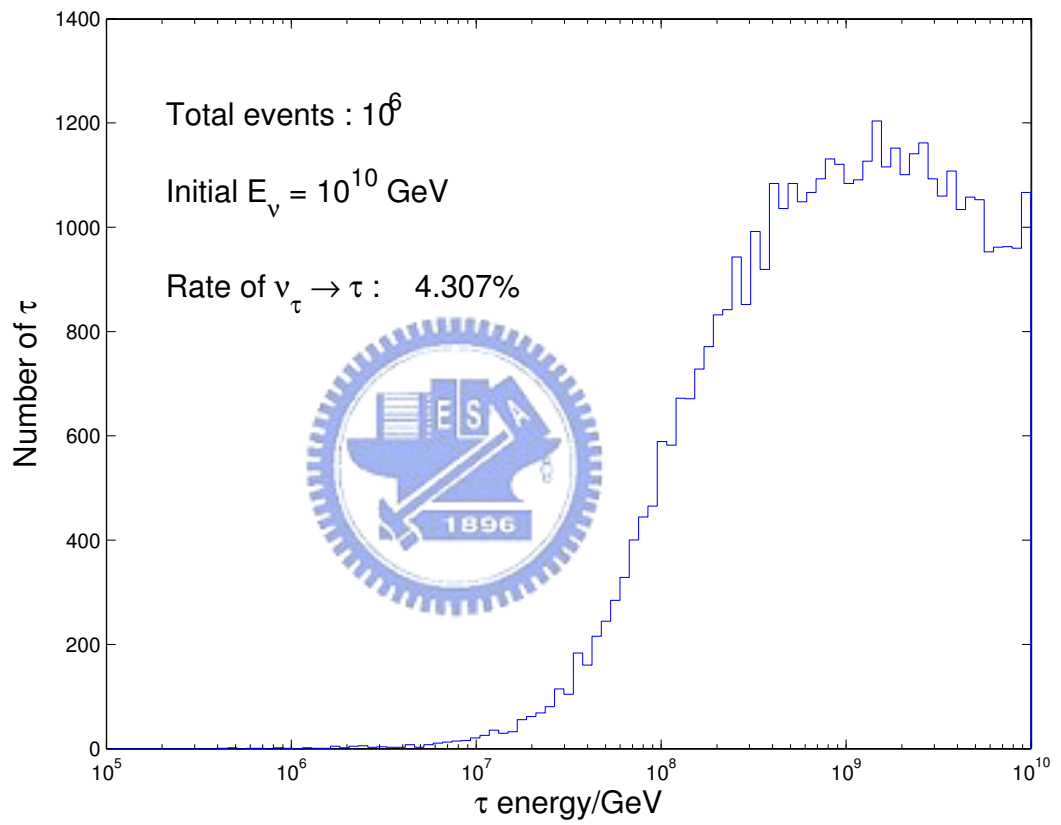


Figure 21: Tau-lepton energy distribution for multiple-interaction process. Initial energy of incident  $\nu_\tau$  is  $10^{10}$  GeV and the thickness of standard rock is  $4 \times 10^4$  m.

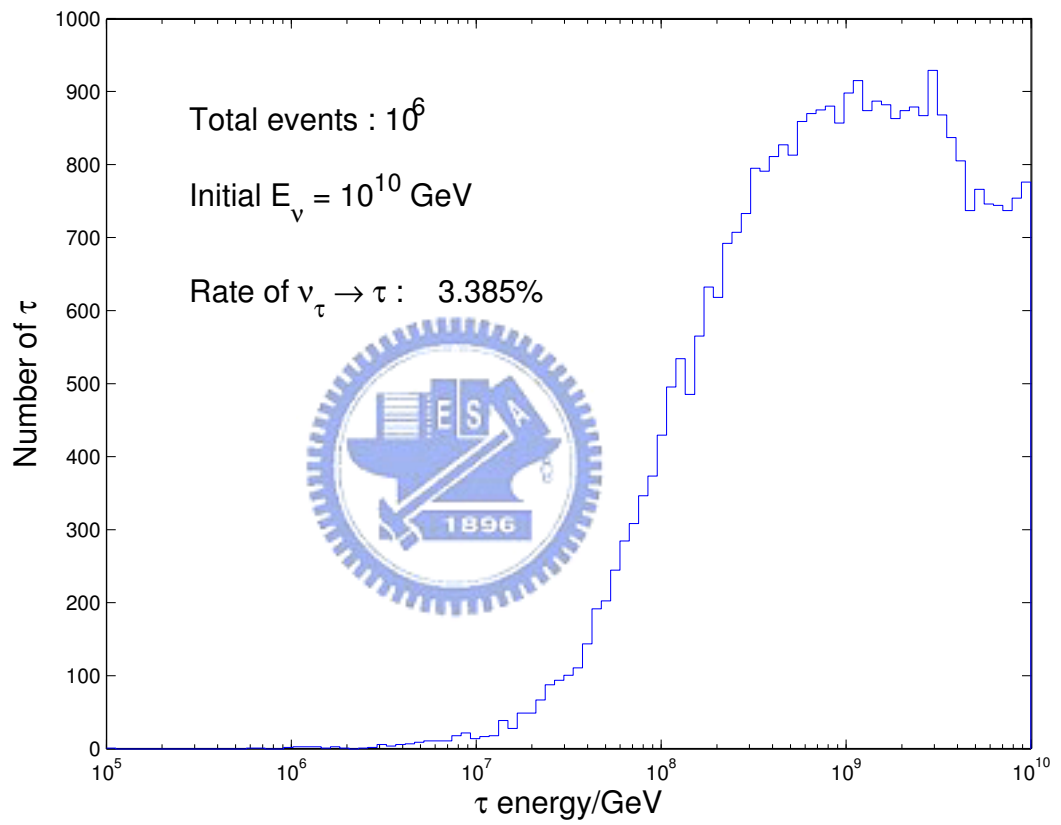


Figure 22: Tau-lepton energy distribution for multiple-interaction process. Initial energy of incident  $\nu_\tau$  is  $10^{10}$  GeV and the thickness of standard rock is  $1 \times 10^5$  m.

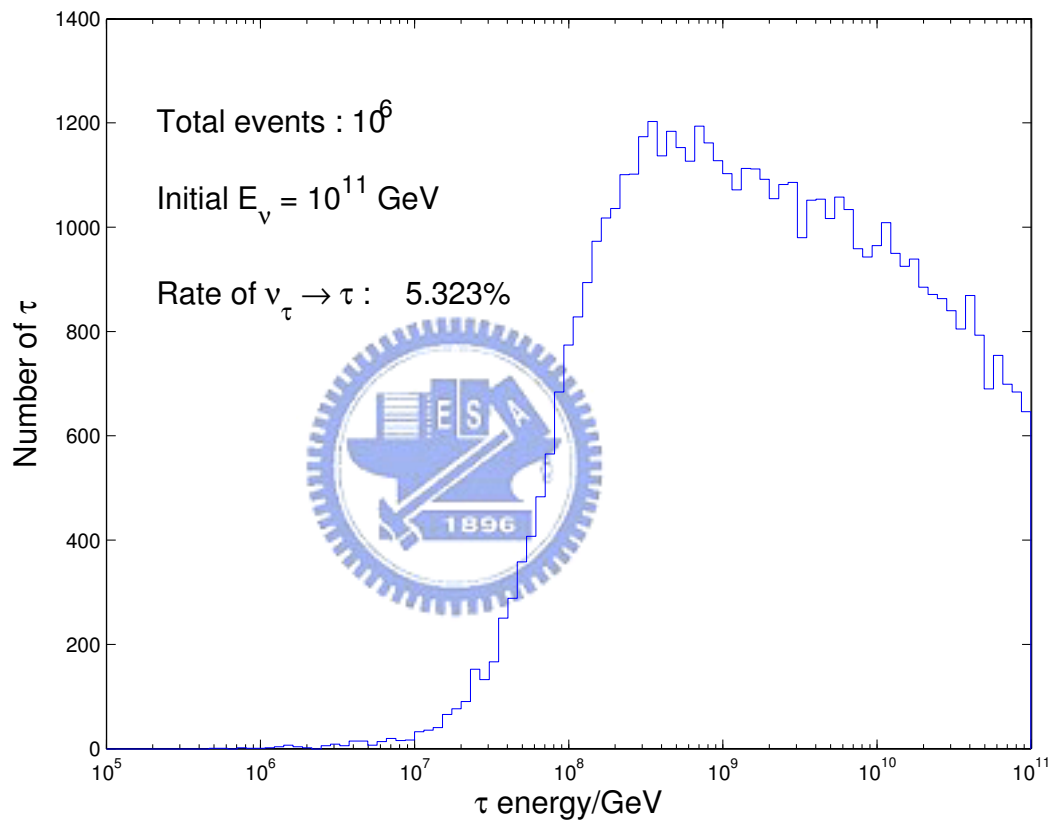


Figure 23: Tau-lepton energy distribution for multiple-interaction process. Initial energy of incident  $\nu_\tau$  is  $10^{11}$  GeV and the thickness of standard rock is  $1 \times 10^5$  m.

The fraction of difference in the tau range is 12.5% when we only consider the pair production loss in the case of  $E_\tau = 10^{10}$  GeV, shown as Fig. 7. It becomes 25% with the adding of the photonuclear loss, shown as Fig. 11. It means that we obtain a different tau range with the Monte-carlo method, especially in the case of high energy tau, Fig. 11.

Next, we consider the incident  $\nu_\tau$  in the finite thickness medium. The exit tau is detected through its induced air showers by the detector placed at some distance from the end of the medium. The  $\nu_\tau \rightarrow \tau$  conversion rate is shown in Fig. 14. Note that the rate is increased with the incident  $\nu_\tau$  energy because that the  $\nu_\tau$  charge-current interaction length is shorter. Thus, the high energy  $\nu_\tau$  flux is easy to scatter and produce  $\tau$  in the medium. Moreover, the high energy tau range is longer and the produced tau may survive until reaching the end of the medium. As a result, the  $\nu_\tau \rightarrow \tau$  conversion rate increases with the  $E_\nu$ .

Next we discuss the relationship between the medium thickness and the  $\nu_\tau \rightarrow \tau$  rate for the  $10^{10}$  GeV incident  $\nu_\tau$ . After we change the medium thickness from  $1 \times 10^5$  m to  $5 \times 10^4$  m and  $2 \times 10^4$  m, the  $\nu_\tau \rightarrow \tau$  rate is increased by about 0.5% and 1%, respectively as shown in Tab. 3. But in the case  $10^7$  GeV, the difference reduced to be about 0.002%, as shown in Tab. 2. One can understand this by the probability density of  $\nu_\tau$  charge-current scattering. In the high-energy  $\nu_\tau$  case, the probability for  $\nu_\tau N$  charge-current scattering is higher and it leads to a decreased  $\nu_\tau$  flux. Thus, the  $\nu_\tau$  flux is decreased with the medium thickness and the tau flux is decreased also. On the contrary, the low energy  $\nu_\tau$  is hard to scatter in the medium and the  $\tau$  flux is independent of the medium thickness.

We estimate the numerical value of the conversion rate. Since we consider the charge-current scattering as a Poisson process, by Eq. (22), the normalized probability density is

$$\frac{dP_{cc}}{dx} = \frac{1}{L_{cc}} e^{-\frac{x}{L_{cc}}}, \quad (60)$$

where  $L_{cc}$  is the charge-current interaction thickness shown in Fig. 1. If the medium thickness is  $L_m$ , the probability that we can obtain the  $\tau$  in the range  $L_m - R_\tau < x <$

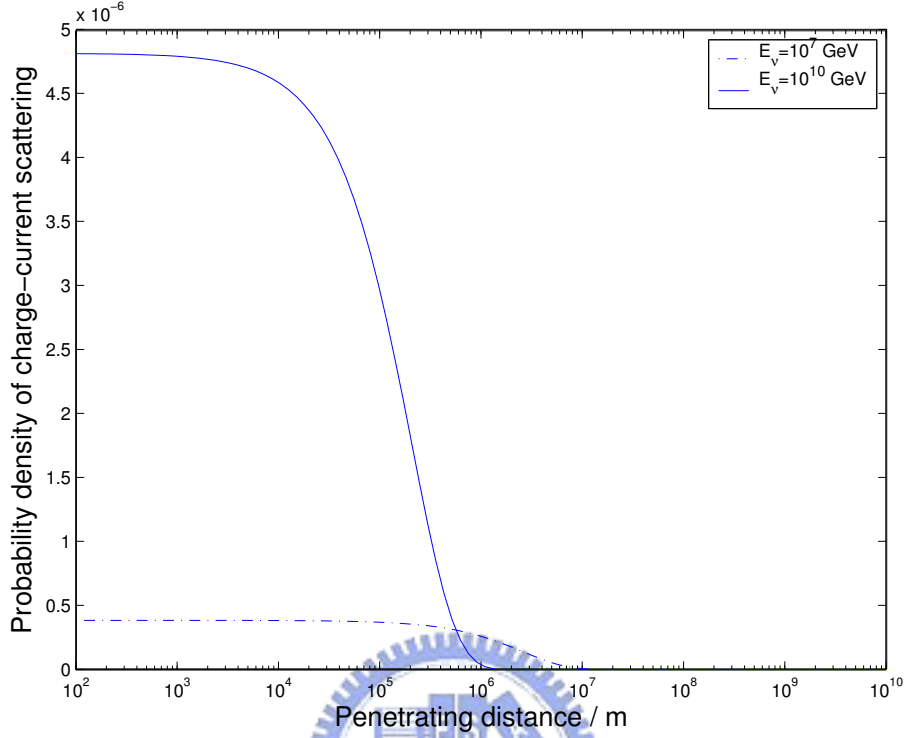


Figure 24: Charge current interaction probability for  $E_\nu = 10^7$  GeV and  $E_\nu = 10^{10}$  GeV.

$L_m$  is

$$P\{L_m - R_\tau < x < L_m\} = \int_{L_m - R_\tau}^{L_m} \frac{1}{L_{cc}} e^{-\frac{x}{L_{cc}}} dx, \quad (61)$$

where  $R_\tau$  is the tau lepton range, which increases with  $E_\tau$ . By approximation, we can pick  $E_\tau = E_\nu$  if we neglect the energy loss of  $\nu_\tau$  scatterings. Since  $L_{cc}$  decrease with  $E_\nu$ , the curve of  $\frac{dP_{cc}}{dx}$  is sharper in high energy case. The  $\frac{dP_{cc}}{dx}$  of  $E_\nu = 10^7$  is lower than the case of  $E_\nu = 10^{10}$  if the penetrating distance is below  $6 \times 10^5$  m, shown as Fig. 24. Therefore, in this low penetrating distance,  $P\{L_m - L_{cc} < x < L_m\}$  increases with  $E_\nu$ .

The tau-lepton range in rock for  $E_\tau = 10^{10}$  GeV is  $1.18 \times 10^4$  m, Fig. 9, and the medium thickness is  $2 \times 10^4$  m. It means that the detector can see the exit  $\tau$  when it is created in the range

$$8.2 \times 10^3 \text{ m} < x < 2 \times 10^4 \text{ m},$$

and the probability is

$$P\{8.2 \times 10^3 \text{ m} < x < 2 \times 10^4 \text{ m}\} = \int_{8.2 \times 10^3 \text{ m}}^{2 \times 10^4 \text{ m}} \frac{1}{L_{cc}} e^{-\frac{x}{L_{cc}}} dx = 5.3\%. \quad (62)$$

Similarly, for the  $5 \times 10^4 \text{ m}$  and  $10^5 \text{ m}$  medium, the probabilities are

$$P\{3.82 \times 10^4 \text{ m} < x < 5 \times 10^4 \text{ m}\} = \int_{3.82 \times 10^4 \text{ m}}^{5 \times 10^4 \text{ m}} \frac{1}{L_{cc}} e^{-\frac{x}{L_{cc}}} dx = 4.58\%, \quad (63)$$

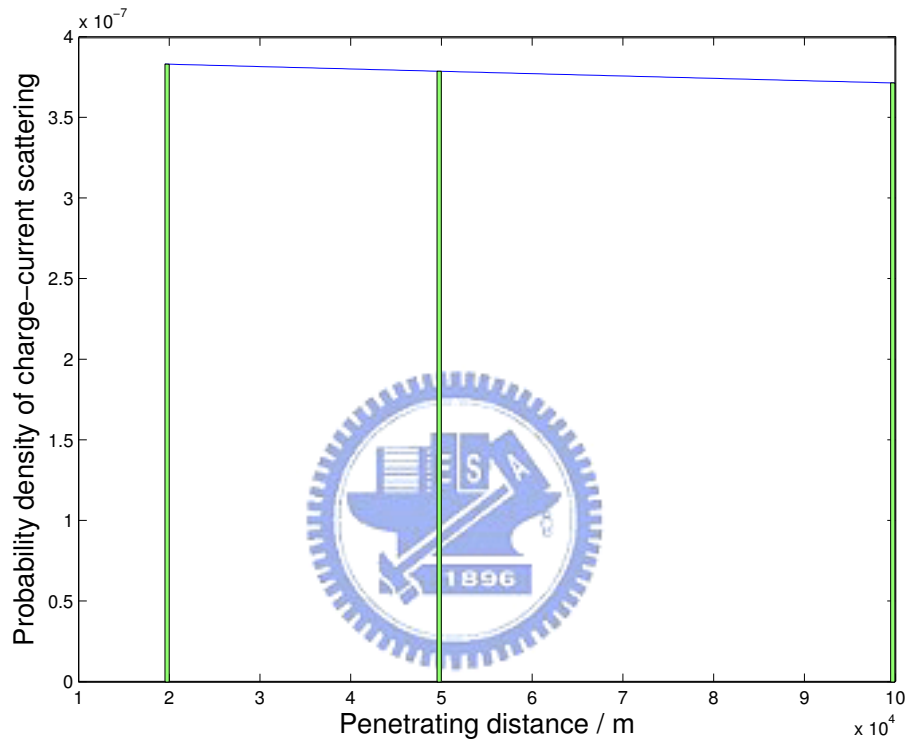
$$P\{8.82 \times 10^4 \text{ m} < x < 10^5 \text{ m}\} = \int_{8.82 \times 10^4 \text{ m}}^{10^5 \text{ m}} \frac{1}{L_{cc}} e^{-\frac{x}{L_{cc}}} dx = 3.6\%. \quad (64)$$

These probabilities are illustrated in Fig. 26. The corresponding for  $E = 10^7 \text{ GeV}$  and  $E = 10^{11} \text{ GeV}$  can be found in Fig. 25, 27.

The difference of these three probabilities are 0.7% and 0.98%. This is consistent with the results shown by Tab. 3. We conclude that the decreasing of  $\nu_\tau \rightarrow \tau$  rate with increasing medium lengths is caused by the decreasing of the charge-current scattering probability. Furthermore, we can explain why the difference is smaller in  $E = 10^7 \text{ GeV}$  in Tab. 2. We only need to focus on the changes of  $L_{cc}$  and the tau range. For a larger  $L_{cc}$ , the slope of  $\frac{dP_{cc}}{dx}$  is reduced and the differences for integrals in Eq. 61 with respect to different regions are decreased also. This is the reason why the difference of rate in Tab. 2 is lower than in Tab. 3.

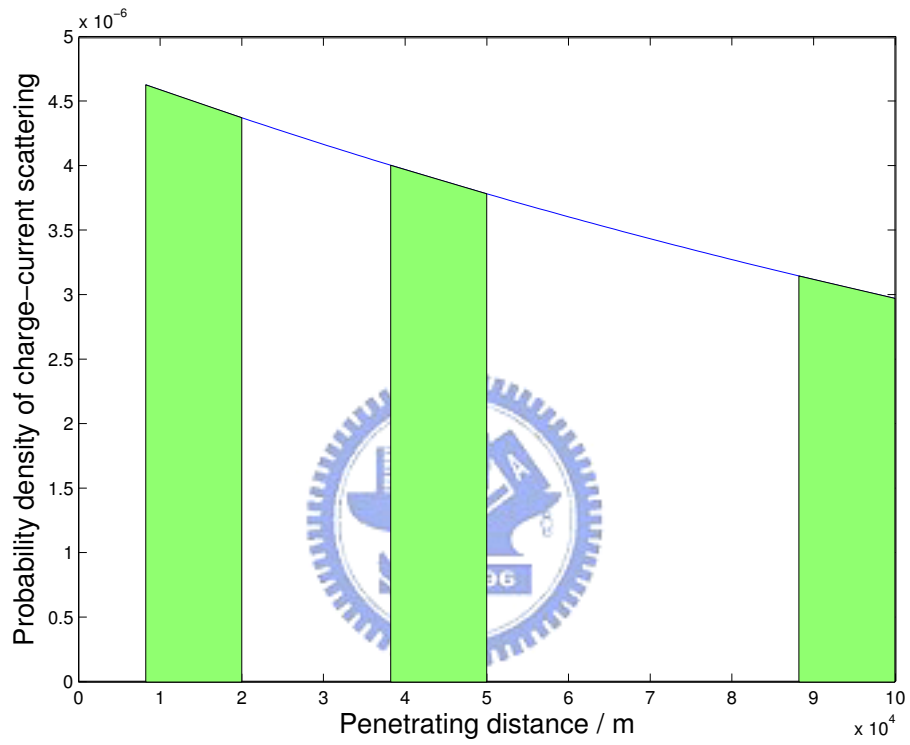
In all energy spectra, Fig.15-23, the number of  $\tau$  decreases rapidly in the energy region below  $10^8 \text{ GeV}$  and it is independent of the initial energy of  $\nu_\tau$ . It is due to the fact that  $\tau$  decay easily when its energy is below  $10^8 \text{ GeV}$ .

Finally, a plateau can be found in the  $\tau$  energy spectra arising from ultra-high energy initial  $\nu_\tau$ , Fig. 23. It means that we cannot easily identify the energy of the original high-energy  $\nu_\tau$ , unless a huge number of  $\tau$  are detected. On the other hand, the energy spectra of low energy source is sharp whereas the  $\nu_\tau \rightarrow \tau$  conversion rate is too low. So it is hard to detect enough events for data analysis in this case.



Thickness of medium / m	Probability
$2 \times 10^4$ m	0.0178%
$5 \times 10^4$ m	0.0176%
$1 \times 10^5$ m	0.0172%

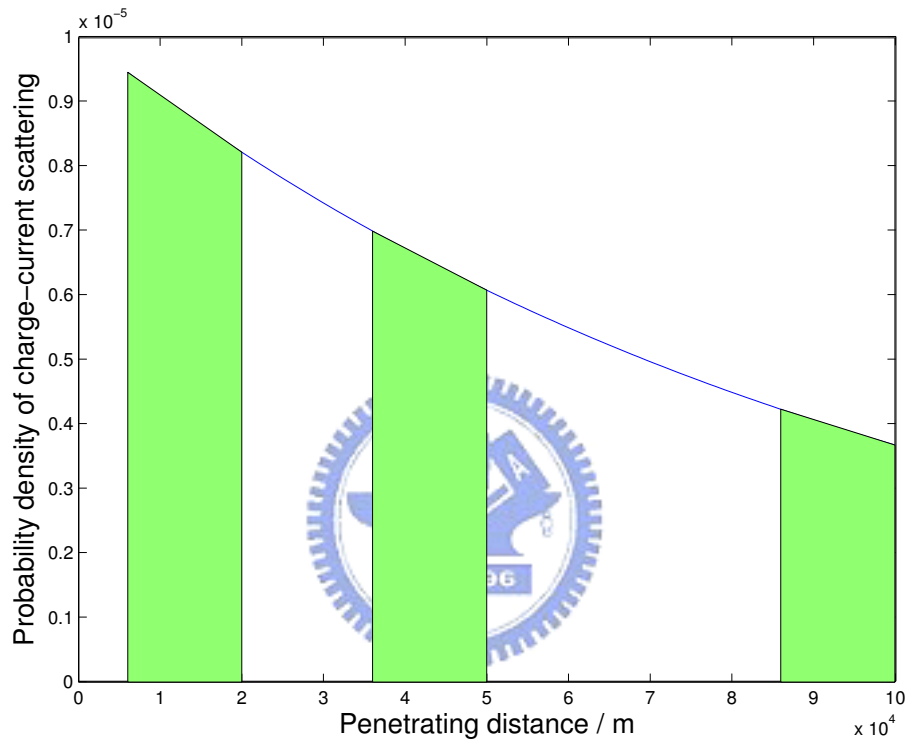
Figure 25: The probabilities of charge current scattering for  $E_\nu = 10^7$  GeV, the three regions of integral area are the probabilities of medium with  $2 \times 10^4$ m,  $5 \times 10^4$ m,  $1 \times 10^5$ m.



Thickness of medium / m	Probability
$2 \times 10^4$ m	5.30%
$5 \times 10^4$ m	4.58%
$1 \times 10^5$ m	3.60%

Figure 26: The probabilities of charge current scattering for  $E_\nu = 10^{10}$  GeV, the three regions of integral area are the probabilities of medium with  $2 \times 10^4$ m,  $5 \times 10^4$ m,  $1 \times 10^5$ m.





Thickness of medium / m	Probability
$2 \times 10^4$ m	12.33%
$5 \times 10^4$ m	9.12%
$1 \times 10^5$ m	5.52%

Figure 27: The probabilities of charge current scattering for  $E_\nu = 10^{11}$  GeV, the three regions of integral area are the probabilities of medium with  $2 \times 10^4$ m,  $5 \times 10^4$ m,  $1 \times 10^5$ m.

## 7 Conclusion

We have studied the behavior of  $\nu_\tau$  and  $\tau$  in standard rock by applying the Monte-carlo method. Unlike the deterministic method, the  $\tau$  energy distribution resulting from the propagation of single-energy tau-neutrinos can be obtained in this way. The Monte-carlo method also gives a shorter tau-lepton range. Furthermore, we have tried to explain the relationship between the  $\nu_\tau \rightarrow \tau$  rate and the medium thickness in Sec. 6. A challenge for  $\nu_\tau$  energy resolution is presented. The task to reconstruct the original  $\nu_\tau$  energy is non-trivial due to the plateau of the  $\tau$  energy spectra.

## References

- [1] S. Iyer Dutta, M. H. Reno, I. Sarcevic, and D. Seckel, Phys. Rev. D 63, 094020 (2001).
- [2] L. Pasquali and M. H. Reno, Phys. Rev. D 59, 093003 (1999).
- [3] Jie-Jun Tseng, Tsung-Wen Yeh, H. Athar, M. A. Huang, Fei-Fain Lee, and Guey-Lin Lin, Phys. Rev. D 68, 063003 (2003).
- [4] Raj Gandhi, Chris Quigg, Mary Hall Reno, and Ina Sarcevic, Phys. Rev. D 58, 093009 (1998).
- [5] Paolo Lipari, and Todor Stanev, Phys. Rev. D 44, 3543 (1991)
- [6] R. P. Kokoulin and A. A. Petrukhin, in Proceedings of the XII International Conference on Cosmic Rays, Vol. 6.
- [7] L. B. Bezrukov and E. V. Bugaev, Yad. Fiz. 33, 1195 (1981)
- [8] Erhan Cinlar, Introduction to stochastic processes.

## List of Figures

- 1 Charge current scattering thickness in standard rock. . . . . 12

2	The distribution of $y$ for the $\tau$ decay processes. . . . .	14
3	The tau-lepton penetrating distance in the standard rock considering only decay (without energy loss interaction). Initial tau-lepton energy is $10^{10}$ GeV. The exponential decay constant is about $-2 \times 10^{-6}/\text{m}$ . . . . .	19
4	Tau-lepton range considering only the decay process. . . . .	20
5	The tau-lepton penetrating distance inside the standard rock considering the pair production interaction. Initial energy of $\tau$ is $10^{10}$ GeV. . . . .	21
6	Tau-lepton range considering the pair production interaction. . . . .	22
7	The fraction of difference in the tau-range between the Monte-carlo method and the deterministic method. The comparison is made by considering only the pair-production loss. . . . .	23
8	The tau-lepton penetrating distance inside the standard rock considering the pair production and photonuclear interactions. Initial energy of $\tau$ is $10^{10}$ GeV. . . . .	24
9	Tau-lepton range considering the pair production and photonuclear interactions. . . . .	25
10	The comparison with the Monte-carlo calculation by Reno [1]. . . . .	26
11	The fraction of difference in the tau-range between the Monte-carlo method and the deterministic method. The comparison is made by considering the pair-production and photonuclear losses. . . . .	27
12	Tau-lepton energy distribution for the single-interaction process. Initial energy of incident $\nu_\tau$ is $10^8$ GeV. . . . .	28
13	Tau-lepton energy distribution for the single-interaction process. Initial energy of incident $\nu_\tau$ is $10^{10}$ GeV. . . . .	29
14	The conversion percentage for $\nu_\tau \rightarrow \tau$ in a single-interaction process with the medium length $10^5$ m. . . . .	30
15	Tau-lepton energy distribution for multiple-interaction process. Initial energy of incident $\nu_\tau$ is $10^7$ GeV and the thickness of standard rock is $2 \times 10^4$ m. . . . .	32

16	Tau-lepton energy distribution for multiple-interaction process. Initial energy of incident $\nu_\tau$ is $10^7$ GeV and the thickness of standard rock is $5 \times 10^4$ m. . . . .	33
17	Tau-lepton energy distribution for multiple-interaction process. Initial energy of incident $\nu_\tau$ is $10^7$ GeV and the thickness of standard rock is $1 \times 10^5$ m. . . . .	34
18	Tau-lepton energy distribution for multiple-interaction process. Initial energy of incident $\nu_\tau$ is $10^8$ GeV and the thickness of standard rock is $1 \times 10^5$ m. . . . .	35
19	Tau-lepton energy distribution for multiple-interaction process. Initial energy of incident $\nu_\tau$ is $10^9$ GeV and the thickness of standard rock is $1 \times 10^5$ m. . . . .	36
20	Tau-lepton energy distribution for multiple-interaction process. Initial energy of incident $\nu_\tau$ is $10^{10}$ GeV and the thickness of standard rock is $2 \times 10^4$ m. . . . .	37
21	Tau-lepton energy distribution for multiple-interaction process. Initial energy of incident $\nu_\tau$ is $10^{10}$ GeV and the thickness of standard rock is $4 \times 10^4$ m. . . . .	38
22	Tau-lepton energy distribution for multiple-interaction process. Initial energy of incident $\nu_\tau$ is $10^{10}$ GeV and the thickness of standard rock is $1 \times 10^5$ m. . . . .	39
23	Tau-lepton energy distribution for multiple-interaction process. Initial energy of incident $\nu_\tau$ is $10^{11}$ GeV and the thickness of standard rock is $1 \times 10^5$ m. . . . .	40
24	Charge current interaction probability for $E_\nu = 10^7$ GeV and $E_\nu = 10^{10}$ GeV. . . . .	42
25	The probabilities of charge current scattering for $E_\nu = 10^7$ GeV, the three regions of integral area are the probabilities of medium with $2 \times 10^4$ m, $5 \times 10^4$ m, $1 \times 10^5$ m. . . . .	44

26	The probabilities of charge current scattering for $E_\nu = 10^{10}$ GeV, the three regions of integral area are the probabilities of medium with $2 \times 10^4$ m, $5 \times 10^4$ m, $1 \times 10^5$ m. . . . .	45
27	The probabilities of charge current scattering for $E_\nu = 10^{11}$ GeV, the three regions of integral area are the probabilities of medium with $2 \times 10^4$ m, $5 \times 10^4$ m, $1 \times 10^5$ m. . . . .	46

